The Journal of Neuroscience, November 1, 1997, 17(21):8408–8426

Transition from Growth Cone to Functional Motor Nerve Terminal in *Drosophila* Embryos

Motojiro Yoshihara,[1] Mary B. Rheuben,[2] and Yoshiaki Kidokoro[1]

[1]*Gunma University School of Medicine, Maebashi 371, Japan, and* [2]*Department of Anatomy, College of Veterinary Medicine, Michigan State University, East Lansing, Michigan 48824*

As a motor axon grows from the CNS to its target muscle, the terminal has the form of a flattened growth cone with a planar central region, lamellipodia, and filopodia. A mature terminal usually has a stereotyped shape that may be elongated with varicosities, as in several invertebrate species, or have short branches with boutons, as in mammals. We examined in *Drosophila* the developmental changes between growth cone and mature terminal using ultrastructural and immunocytochemical methods.

The transition period, which occurs 2–3 hr after the first growth cone reaches its target muscle, is marked by the formation of "prevaricosities," smoothly contoured enlargements of the axons at the point where the nerve trunk first contacts the muscle fiber (MF). There is a 15–30 min ventral-to-dorsal gradient in the formation of prevaricosities on the individual abdominal MFs. Multineuronal innervation of each MF has occurred by this time, and two or more different axons undergo prevaricosity formation while they are intimately intertwined at the nerve entry point (NEP). Presynaptic active zones, both nerve–nerve and nerve–muscle, occur within the prevaricosities along broad contact regions. Synaptotagmin immunoreactive clusters form concurrently.

The first varicosities then develop as a result of constrictions of the larger prevaricosities rather than as enlargement of discrete portions of the filopodia or neurites. The prevaricosity stage therefore may include the key steps that lead to the differentiation of functional differences in terminal subtypes as well as those leading to the formation of a stable neuromuscular junction.

Key words: Drosophila; *neuromuscular junction; synaptogenesis; growth cone; development; immunohistochemistry*

Mature neuromuscular junctions of various species are characterized by long, infrequently branched nerve terminals, chains of varicosities, or clusters of boutons that house the specializations associated with fast, high quantity transmitter release and recycling. Quantitative variations in that morphology, both characteristic and plastic, are associated with changes in functional capabilities (for review, see Atwood and Wojtowicz, 1986; Hall and Sanes, 1993; Burns and Augustine, 1995).

In *Drosophila* the subtypes of larval motor terminals have varicosities of characteristic dimensions and cytoplasmic inclusions (Johansen et al., 1989a; Atwood et al., 1993; Jia et al., 1993). Mutations that produce defects in neuronal proteins can directly or indirectly affect terminal shape. For example, mutations that modify the properties of excitable channels, thus altering the level of neuronal activity, also change the number of branches and the number of varicosities in mature terminals (Budnik et al., 1990). Similarly, the effect of altered cAMP levels (Zhong et al., 1992), adhesion molecules such as Fasciclin II (Fas II) (Schuster et al., 1996b; Stewart et al., 1996), and specific synaptic proteins such as syntaxin (Broadie et al., 1995) all result in a change in the number of varicosities formed. In some mutants this is independent of the resulting synaptic strength and may be accompanied by changes in numbers of synaptic structures within the varicosity as well (Jia et al., 1993; Stewart et al., 1996). These mutants thus offer clues as to the mechanisms underlying plasticity.

A motor nerve terminal during outgrowth from the CNS has the form of a growth cone, a flared veil-like enlargement of the axon tip with numerous exploring filopodia, in *Drosophila* (Goodman et al., 1984) as well as in vertebrates (Ramon y Cajal, 1890; Harrison, 1910). Growth cones explore among potential MF targets and connect only to specific ones (Johansen et al., 1989b; Halpern et al., 1991; Sink and Whitington, 1991; Van Vactor et al., 1993). A growth cone has given rise to a varicose terminal characteristic of the specific MF, albeit with fewer than the mature number of varicosities, by the time the embryo hatches (Halpern et al., 1991; Broadie and Bate, 1993). However, little is known about the interactions between a growth cone and an MF that determine the final placement of the terminal on a specific part of the selected fiber, the exchange of the labile form of the growth cone for the characteristic branch pattern, or those that determine varicosity size and varicosity number.

To begin an analysis of these steps we examined the cellular reorganization that occurs during the transition from the growth cone to terminal in specified abdominal MFs in *Drosophila* embryos. This period coincides with the time that miniature excita-

Received May 14, 1997; revised Aug. 22, 1997; accepted Aug. 22, 1997.

This work was supported by Grants-in-Aid from the Ministry of Education, Science, Sports, and Culture to Y.K. and M.Y., grants from the Brain Science Foundation and Kato Memorial Science Foundation to M.Y., an All-University Research Initiation Grant from Michigan State University, and grants from the Narishige Neurosciences Foundation and the Yamada Science Foundation to M.B.R., and from the Mitsubishi Foundation to Y.K. We thank Dr. Kazuo Ikeda and Dr. Masahiro J. Go for kind instruction, Dr. Hugo Bellen for the antibody to synaptotagmin, and Dr. Michihiro Igarashi, Dr. Kensuke Hayashi, Dr. Ryoki Ishikawa, Dr. Kei Ito, and Dr. Hiroshi Kuromi for useful discussions. The confocal studies were performed in Dr. Harunori Ishikawa's laboratory, and we thank him and the members of his lab for kind help. We also gratefully acknowledge the technical assistance of Dawn Autio, Jessica Hoane, Nobuko Yoshihara, Fumiko Sekiguchi, and Masako Terada, as well as Takeshi Masuda and Kouei Suto of the Gunma University electron microscope facility.

M.Y. and M.B.R. contributed equally to this research.

Correspondence should be addressed to Dr. Mary B. Rheuben, Department of Anatomy, A514 East Fee Hall, Michigan State University, East Lansing, MI 48824.

 0270-6474/97/178408-19$05.00/0

tory junctional currents are first recorded (Broadie and Bate, 1993; Kidokoro and Nishikawa, 1994) and therefore includes the synaptic activity important to modulating terminal morphology. We describe a transitional structure containing organelles associated with transmitter release, whose shape first presages the branch pattern of the mature terminal but whose dimensions are larger than those of mature varicosities.

MATERIALS AND METHODS

Fly stocks. For all specimens in this study, we used wild-type *Drosophila melanogaster*, strain Canton-Special. The stock was maintained using standard fly-rearing techniques (Ashburner, 1989). The artificial diet contained cornmeal, sugar, yeast, and agar. Incubator temperatures were kept at 25 ± 1°C and humidity at >50%, and the flies were reared under uncrowded conditions.

Staging. For the precisely timed embryos needed for the developmental studies, adult male and female flies were placed into a bottle with an agar plate in the bottom and allowed to lay eggs in the incubator for 1 hr. A paste consisting of 1 gm of dry yeast and 1.5 ml grape juice was placed on the surface of the agar plate to stimulate egg laying. After a precollection period of 1 hr, the agar plate was exchanged for a new one, and flies were allowed to lay eggs for 10 min. This plate was then transferred to a moist chamber for embryonic development. The temperature was precisely controlled at 25 ± 0.5°C for egg laying and subsequent development. Thus, the hours after egg laying (AEL) were accurately timed within ~5 min and were approximately the same as hours after fertilization. Under these conditions, embryos develop synchronously and hatch at approximately 21 hr AEL (Broadie and Bate, 1993). The morphology of the intestine, color of Malpighian tubules, presence of air in tracheae, cuticle formation, and ability to move were also used to confirm stage of development. For the electron microscopy studies, eggs were collected over 30 min time periods.

Preparation and dissection. Embryos and first instar larvae were dissected in an osmotically balanced saline (modified from Stewart et al., 1994), 70 mM NaCl, 20 mM KCl, 25 mM $MgCl_2$, 10 mM $NaHCO_3$, 2 mM NaH_2PO_4, 5 mM L-glutamine, 5 mM trehalose, 40 mM sucrose, 10 mM HEPES buffer, pH 7.1.

Before 17 hr AEL, when the epidermis still stuck to glass, a "flat preparation" was made according to Bate's method in Ashburner (1989). Briefly, mechanically dechorionated embryos were placed on a double-side sticky tape. The vitelline membrane was cut with a sharp glass needle; the embryo was removed from it and put on a clean glass slide. The body wall was cut longitudinally along the embryo's left side with a glass needle and then uncurled so that its outer surface stuck to the glass slide. The intestine, fat body, and tracheae were removed with fine forceps or sucked away with a fine glass capillary tube.

After 17 hr AEL, dissection was performed with a pair of sharpened needles using a method modified from Kidokoro and Nishikawa (1994). The posterior end of the embryo was immobilized by one needle and pierced with a second needle that was ground in the shape of a knife. Then, the knife needle was inserted deeply into the abdomen, and the body wall (epidermis and muscles) along the left side of the animal was cut by pushing the animal against the bottom of the dish. Care was taken not to damage the right side or the nervous system. Dissected embryos and first instar larvae were mounted on Lux 13 mm Thermanox coverslips (Nunc, Naperville, IL) using single strands of dragline spider silk. The main support strands of spider webs are not sticky and can be dissociated into individual fibers of sufficient strength and elasticity to bind the filleted embryo to the coverslip. We used silk from *Nephila clavata*, a common Japanese spider. The strands of web were inserted into notches cut in the edges of the plastic coverslips, and their placement was adjusted to suit the size of the larva being immobilized. This particular type of coverslip and the spider web could be carried through fixation, dehydration, and embedding without damage, or could be used as the support planchette for critical point drying and examination in the scanning electron microscope. Wells were made around the specimens to further protect them from mechanical damage by gluing a second coverslip, with a 4 × 2 mm rectangular hole cut out of the center, over the coverslip holding the web. For some transmission electron microscopy (TEM) samples, 1–4% agarose (gelling temperature 25°C) (Boehringer Mannheim, Indianapolis, IN) was poured over the sample just before the end of aldehyde fixation and then hardened, and fixation finished [modified from Wood and Klomparens (1993)]. The solidified and fixed agarose block containing the specimen was cut free from the spider web strands just before embedding. Third instar larvae were held to coverslips either with dental floss or fine wire or in some instances were carried part way through preparation pinned to Sylgard (Dow Corning, Midland, MI) in a 35 mm petri dish.

Some embryos were prepared for TEM without dissection to minimize the damage that occurs during filleting. Undissected animals were perfused directly with fixative via a glass micropipette inserted into the posterior abdomen, with a second small hole in the epidermis having been made anteriorly for exit of the solution. In a control series examined confocally, two sets of embryos were prepared with and without dissection, and with or without Ca^{2+} in the saline and fixative to assess the effects of mechanical damage and other factors that might affect fragile embryonic structures. None of these treatments affected the appearance of the prevaricosity in animals at the prevaricosity stage (~16.5 hr AEL). However, as noted in the results section, cutting the intersegmental nerves (ISNs) did result in the formation of abnormal-appearing balloon-like prevaricosities on the affected side.

Protocols for fluorescence immunohistochemistry. Dissected preparations were fixed in 4% formaldehyde (made from a 37% solution) in PBS (10 mM Na_2HPO_4 and 130 mM NaCl are mixed with 10 mM NaH_2PO_4 and 130 mM NaCl and titrated to pH 7.2) for 2 hr and washed in PBT (PBS with 0.5% Triton X-100). Goat anti-HRP IgG conjugated to fluorescein (Cappel, Durham, NC) was used for staining all neural cells (Jan and Jan, 1982). After blocking for 1 hr with 1% BSA in PBT, fixed preparations were incubated in antibody solution (1:100 dilution for FITC anti-HRP and 1% BSA in PBT) for 2 hr at room temperature with gentle agitation.

Synaptotagmin was localized by rabbit polyclonal antiserum against synaptotagmin (Littleton et al., 1993), which was kindly provided by Dr. Hugo Bellen. For double-labeling experiments with both synaptotagmin antisera and anti-HRP IgG, fixed and BSA-blocked preparations as above were incubated in primary antibody solution (1:500 dilution for anti-synaptotagmin; 1:100 dilution for FITC anti-HRP and 1% BSA in PBT) for 2 hr at room temperature with gentle agitation. After it was washed in PBT, the preparation was incubated in secondary antibody solution [1:500 dilution for Cy3-conjugated goat anti-rabbit IgG (Chemicon, Temecula CA) and 1% BSA in PBT] for 2 hr at room temperature with gentle agitation and washed again with PBT.

All preparations after staining were mounted with 5% *n*-propyl gallate and 90% glycerol in PBS on a glass slide.

Confocal microscopy. We used an MRC-600 laser scanning confocal microscope (Bio-Rad, Watford, Herts, England) on an Axiophot microscope (Carl Zeiss). The objective lens was a Zeiss Plan-APOCHROMAT 100×/1.3 NA oil immersion iris. We used an argon laser and a filter set for FITC (passing wavelengths of 488 nm for excitation), or for double excitation, we used an argon laser of 514 nm for excitation and a filter set for double labeling. Optically sectioned images were taken at 0.32 μm intervals. Stereo pairs were made at ±9° separation by COMOS software bundled with the MRC-600. *x-z* sections were made from the *x-y* optical section stack by calculation with Thruview software (Bio-Rad).

Measurement of the thickness of synaptic terminals. We examined the thickness of swellings in developing synaptic terminals as follows. First, by systematically changing focus, we found the region of a prevaricosity in the *x-y* coordinates where the distance between the highest in-focus optical section and the lowest in-focus section was the greatest. Then we determined from the computed number of sections at that point whether that depth was >2 μm. By this criterion, the "thickness" of the early, sheet-like growth cone never exceeded 2 μm, but at later stages well defined thickenings were observed. Thus, this method is reasonable for quantitative estimation of the presence of prevaricosities but is not necessarily a measurement of the actual thickness of the terminals.

For measurement of thickness of the terminal swellings of MFs 6 and 7, where the growth cone is disposed perpendicular to the plane of optical section, each *x-y* section was examined to determine the dimensions of the terminal at the region of greatest diameter.

Fixation protocols for electron microscopy. In the most frequently used protocol, specimens intended for electron microscopy were dissected in the calcium-free saline described above, pH 7.2, modified from *Drosophila* saline recipes used by Stewart et al. (1994) and those used by Sonea and Rheuben (1992) on *Manduca* larvae. Solutions over the specimens were first changed to a fixative containing 4% paraformaldehyde, 1% glutaraldehyde in 0.1 M cacodylate or NaH_2PO_4 buffer (Millonig's "C") for 10 min, and then changed to fresh fixative of the same composition

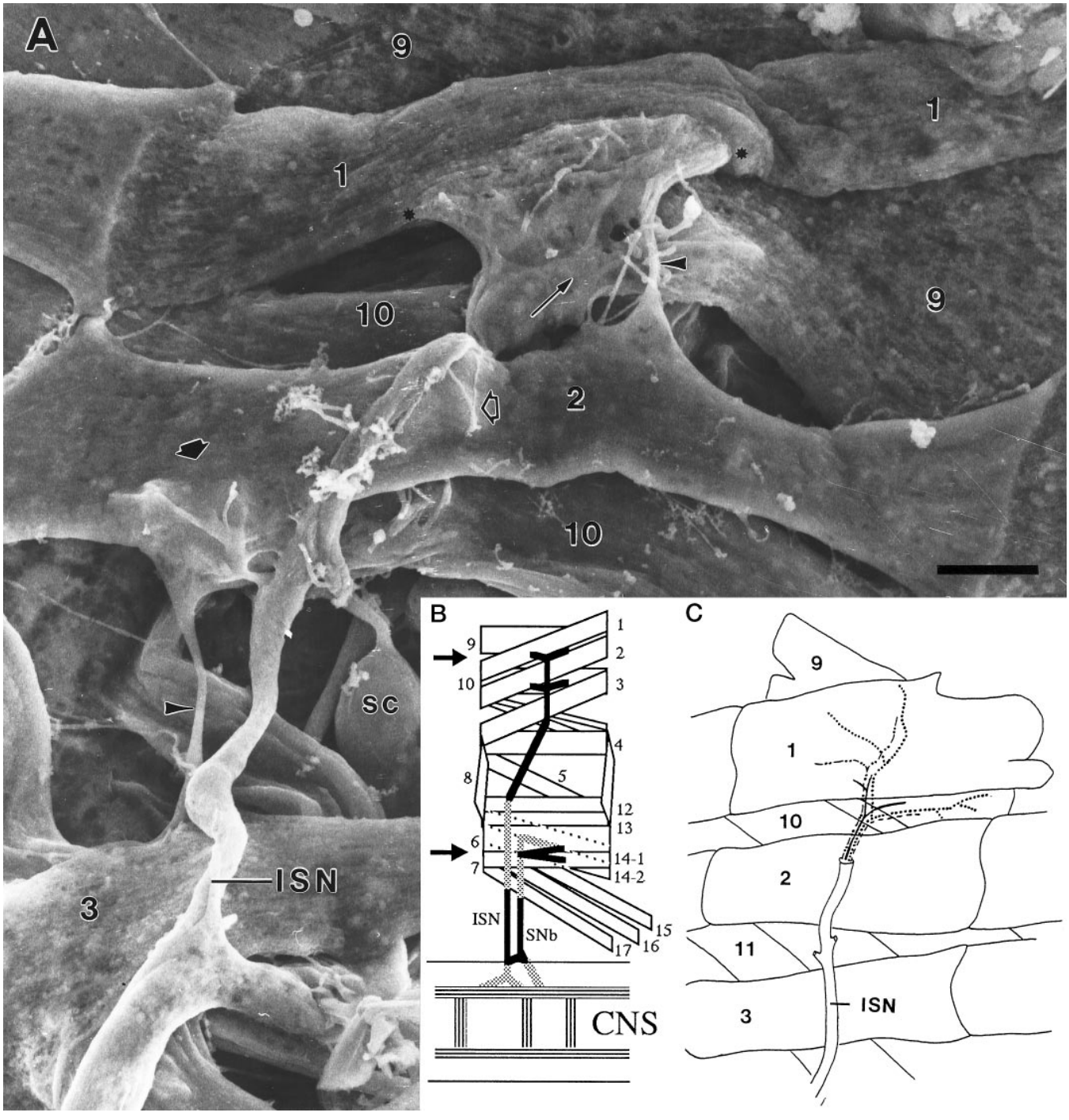

Figure 1. *A*, Scanning electron micrograph of the dorsal abdominal muscles, right side, from an embryo 16.75 hr AEL. Anterior is to the *left*. Compare with *B* and *C*. The ISN crosses over MFs 3 and 2, innervating them in passing, to form a final bifurcation (*thin arrow*) to innervate MFs 1 and 9. The junctional aggregates (the one on MF 1 is *bracketed* between *asterisks*) typify those seen late in the growth cone period or early in the prevaricosity period. On MF 1 the terminals/growth cones are spread out and partially overlapping. They are still relatively flat. An isolated terminal on MF 2 (*short arrow*) illustrates the thickening and swelling of branch near the NEP that is characteristic of the prevaricosity period. Residual MF to MF connections are often seen (*arrowheads*). Filopodia are found both above and below the basal lamina of the MF, and a few are exploring "inappropriate" areas away from the typical junctional sites (*open arrow*), as is also seen in Figure 4*A*. The large lateral sensory cells (*SC*) are exposed between MFs 10 and 3. Prepared with anti-HRP labeling and OTO method. See Figure 2 for interpretation of the method. Photographed at accelerating voltage of 10 kV. Scale bar, 5 μm. *B*, Schematic diagram of a single abdominal segment of a *Drosophila* embryo or larva showing the nomenclature (after Crossley, 1978) and the innervation of the muscles examined in this study. The general innervation pattern is segmentally repeated in abdominal segments A2–A7. Dorsal is to the *top*, and anterior is to the *left*. All subsequent figures illustrating part of an abdominal segment, except Figure 9, are oriented in this manner. The *arrows* indicate the locations of the junctions that were explored. The intersegmental nerve (*ISN*) innervates MFs 1 and 9 primarily on their medial surfaces after its final bifurcation, and segmental nerve b (*SNb*) innervates MFs 6 and 7 along the space between them. *C*, Diagram of the dorsal portion of a typical larval abdominal segment comparable to the region of the embryo shown above. The data available are consistent with an axonal branch pattern such that MFs 1 and 9 share innervation from one large motor axon (*solid line*) and from one Type II axon (*longer dotted line*), but each is innervated by two different motor axons (*dashed lines*), making a total of four axons supplying the two muscles.

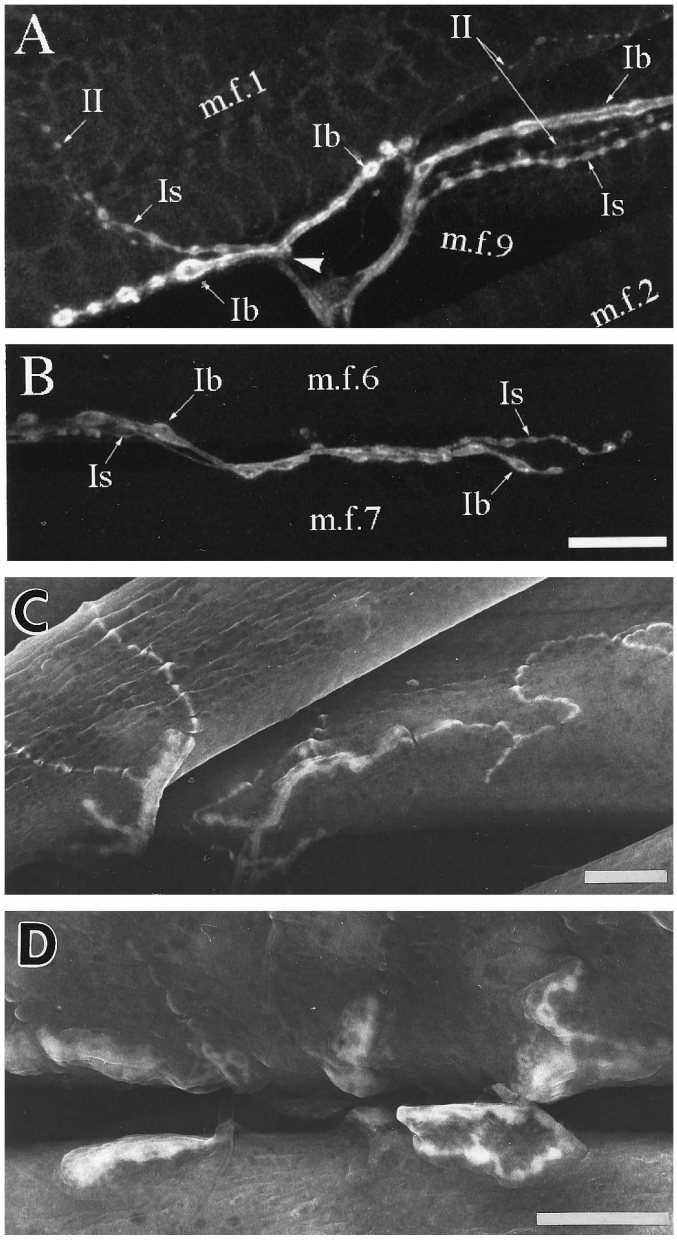

Figure 2. Nerve terminals in mature third instar larvae. In *A* and *B*, nerve cell membranes were stained with fluorescein-tagged anti-HRP, and the projections of confocal optical sections were photographed. For comparison, in *C* and *D* the location of anti-HRP was visualized with DAB and the peroxidase reaction; the precipitate is highly osmiophilic, so labeled structures have enhanced secondary electron emission compared with surrounding tissue in the scanning electron microscope. This method allows clearer visualization of adjacent structures and relationships and is particularly useful in interpreting embryonic structures illustrated subsequently. *A, C*, Three morphological types of nerve terminals innervate MFs 1 (*m.f.1*) and 9 (*m.f.9*). They resemble the Types Ib, Is, and II described on other abdominal muscles (after the nomenclature of Johansen et al., 1989a; Atwood et al., 1993). Each terminal branch consists of a chain of varicosities (boutons) connected by thinner neurites. The terminal types may be distinguished on the basis of the relative sizes of their varicosities, with Ib having the largest varicosities, Is having intermediate-sized varicosities, and II having the smallest varicosities. The terminal branches on MF 9 typically spread posteriorly from the ISN across the medial surface of the fiber. The terminal branches on MF 1 extend both anteriorly and posteriorly; most branches lie on the internal surface of the fiber or along the ventral edge of the fiber, but occasionally some occur on the external surface. The point at which the nerve contacts the edge of MF 1 is indicated by the *arrowhead* in *A*. *B, D*, MFs 6 (*m.f.6*) and 7 (*m.f.7*)

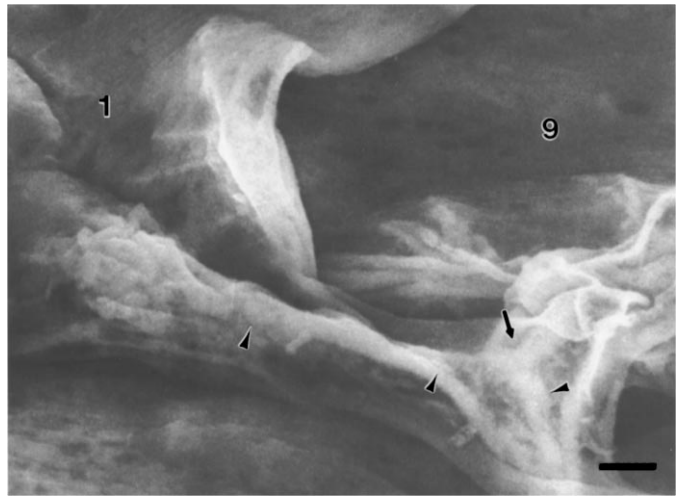

Figure 3. Distal-most bifurcation of the ISN and innervation of MFs 1 and 9 from an embryo 18.5 hr AEL, late in the prevaricosity period. A bifurcation of one of the large motor axons (*thin arrow*) occurs at the point where the ISN divides to innervate MFs *1* and *9*. Small varicosities of the sort typically associated with Type II axons within the nerve trunk are indicated by the *arrowheads*. The junctional aggregate of MF 1 is divided into two parts in this animal, with the right-hand portion forming an enlarged prevaricosity with six shortened filopodia. Both parts appear to be composed of two or more layers of overlapping or intertwined axonal branches. Labeled with anti-HRP, followed by osmium-thiocarbohydrazide treatment. Accelerating voltage, 10 kV. Scale bar, 1 μm.

but containing 0.1 or 0.05 mM Ca^{2+} for an additional 1 or 2 hr (depending on age of specimen) at room temperature. Specimens were then rinsed three times in 0.1 M cacodylate or phosphate buffer from 30 min to overnight at 4°C.

Most of those specimens intended for TEM were post-fixed in 1% OsO_4 in 0.1 M phosphate buffer, 0.05 mM Ca^{2+} for 1 hr, rinsed in phosphate buffer for 30 min, placed in 0.1 M sodium acetate, pH 5.0, for 1 hr, block-stained in 1% UrAc in 50 mM NaAc in the dark for 1.5 hr, dehydrated, and embedded in Epon 812 "hard." Minor variations in this general protocol, including omitting the UrAc block stain, were conducted to improve fixation and staining.

For scanning electron microscopy (SEM), after aldehyde fixation and buffer wash, specimens were transferred gradually (over 1 hr) to distilled water. Modifications of protocols described in Kelley et al. (1973) and Rheuben and Reese (1978) were used to take advantage of the ability of thiocarbohydrazide to enhance osmium binding to cellular organelles, the "OTO" method: after 6 changes in distilled water over at least 1 hr, specimens were placed in 1% OsO_4 for 1–3 hr and then treated with a saturated solution of thiocarbohydrazide (Polysciences, Warrington, PA) in distilled water for 30 min. The sequence of distilled water washes, thiocarbohydrazide, and osmium treatments was repeated up to three times. In some cases, the basal lamina covering the neuromuscular junction was removed first by collagenase digestion (1 mg/ml Type II, Sigma, St. Louis, MO) applied before fixation and again after a post-fixation treatment with 25% KOH for 5 min at 60°C. Treatment times varied because over- and underdigestion were highly unpredictable and occurred even in the same sample. After osmication, samples were washed in distilled water, dehydrated in ethanol, and either critical point-dried through CO_2 or infiltrated with Peldri (Ted Pella, Redding, CA) according to the manufacturer's protocol, frozen, and placed in a vacuum jar for sublimation. Most specimens were examined in the SEM

←

are innervated by Type Is and Ib terminals and usually lack Type II terminals (Atwood et al., 1993). The parts of the junctions extending onto the internal surfaces are easily seen in SEM, but a significant part of the innervation of these two muscles lies within the cleft between them and is extending in a plane perpendicular to the surface. The latter regions can be visualized only if the MFs are rendered transparent, as in fluorescence imaging. Scale bars, 20 μm.

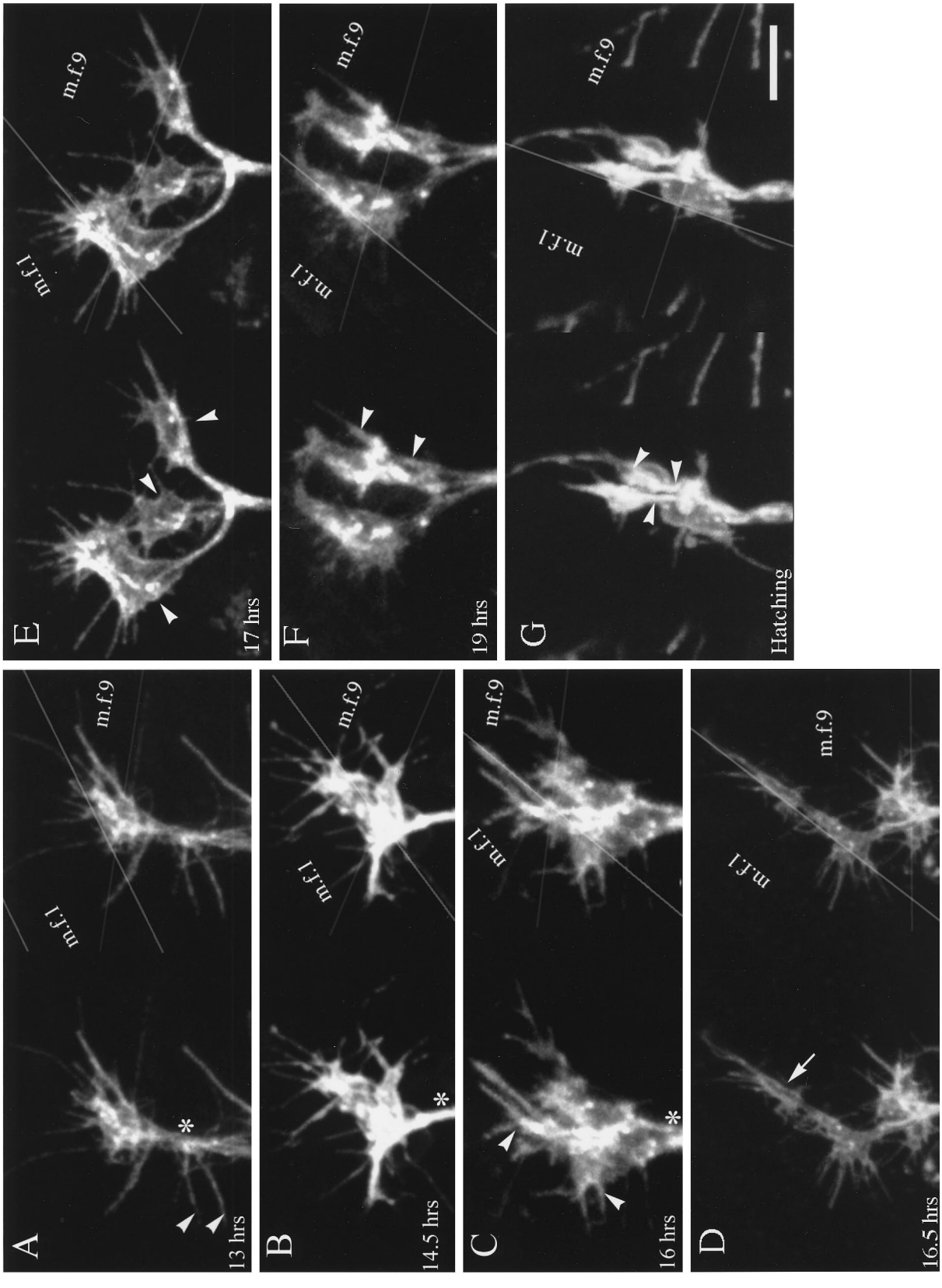

Figure 4. Embryonic development of the innervation of MFs 1 and 9. In each panel, the two confocal images form stereo pairs in the *x-y* plane. The edges of the MFs are indicated by *gray lines* in the right image, and an *asterisk* is placed on the nerve trunk at the point above which all axons would be destined for MFs 1 and 9. Labeling: fluorescein-conjugated secondary antibody to anti-HRP. Scale bar (shown in *G*): 5 μm for all panels. *A*, After the embryonic nerve trunk has reached the dorsal-most target muscles (13 hr AEL). The junctional aggregates of MFs 1 (*m.f.1*) and 9 (*m.f.9*) have a common origin at this developmental stage and consist of one or more overlapping veil-like growth cones that are not distinguishable from one another. It is not possible to determine from these images how many separate axons contribute to the dorsal-most growth cones. Note the (*Figure legend continues*)

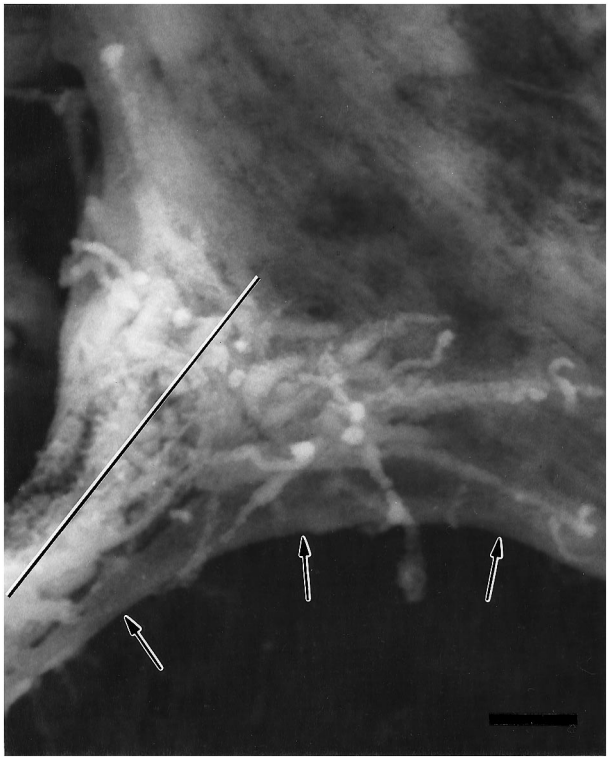

Figure 5. Scanning electron micrograph of an anti-HRP-labeled junctional aggregate at the NEP on MF 1 from an embryo 17 hr AEL, during the prevaricosity period. Processes from two or three of the innervating axons overlie one another. The filopodia are shorter than those seen during the growth cone period, and some axonal branches have begun to enlarge at the NEP. Because the animal was dissected and fixed flat as a "fillet" for SEM, as were the animals examined confocally in Figure 4, we find that the ISN is pulled ventrally and part of the MF membrane (*arrows*) is pulled with it. The plane of section for the junctional aggregate seen in TEM in Figure 6 is indicated by a *line*. Scale bar, 1 μm.

without further treatment after drying; a few (not including those with antibody labels) were coated with a thin layer of platinum to reduce charging.

SEM specimens were photographed at 10–30 kV on either a Hitachi S-800 or an S-4100 field emission microscope with lanthanum hexaboride source in the electron microscopy facility at Gunma University, or with a JEOL 6400 at the Michigan State University Center for Electron Optics. TEM specimens were photographed with a JEOL 100CX or a Phillips CM-10.

Antibody labeling for electron microscopy. To visualize nerve terminal membranes more clearly in SEM, anti-HRP was used. Specimens were fixed with 4% paraformaldehyde in PBS (as described above, pH 7.2) overnight, washed in 0.5% Triton X-100 in PBS (PBT), and incubated in 0.3% H_2O_2 in methanol for 30 min. After a rinse in PBT, specimens were labeled with an antibody to horseradish peroxidase (goat anti-HRP, 1:10,000; Cappel, Durham NC) overnight, and rinsed in PBT. An overnight incubation in biotinylated rabbit anti-goat IgG (H+L) (Vector Laboratories, Burlingame, CA) at a dilution of 1:1000 followed by an overnight incubation in an avidin–biotin complex tagged with HRP (ABC Vectastain Peroxidase Standard, Vector) resulted in amplification of the antibody signal. Specimens were then incubated in a substrate solution containing equal volumes of diaminobenzidine (DAB) (1 mg/ml; Sigma) and 0.02% H_2O_2 in 0.1 M Tris-HCl, pH 7.2, to visualize the reaction product. They were then osmicated and critical point-dried for SEM as described above. Because the DAB reaction product is highly osmiophilic, nervous tissue was more clearly outlined.

Data analysis. The types of terminals were distinguished by criteria derived from the ultrastructural descriptions of third instar larvae provided by Atwood et al. (1993) and Jia et al. (1993) and are consolidated as follows: Type Ib (CV) terminals have 2–5 μm boutons, 44 nm clear-cored vesicles, active zones with T-shaped, branched dense bodies, and a deep subsynaptic reticulum. Type Is (CVo) terminals have somewhat smaller varicosities, clear-cored vesicles of a greater range of sizes, occasional dense-cored vesicles, similar presynaptic dense bodies, and a shallower subsynaptic reticulum. Type II (MV) terminals have varicosities <2 μm, a mixture of clear- and dense-cored vesicles, with the latter being elliptical or irregularly shaped, and they lack a subsynaptic reticulum. Type III (DV) terminals are thought to contain peptides such as an insulin-like peptide on MF 12 (Anderson et al., 1988; Gorczyka et al., 1993) or a leucokinin I immunoreactive peptide on MF 8 (Cantera and Nassel, 1992); they are characterized by a population of large spherical dense-cored vesicles and clusters of small, 33 nm clear vesicles at what appear to be active zones (Jia et al., 1993).

RESULTS

The body wall muscles of *Drosophila* larvae are composed of single identifiable fibers arranged in a segmentally repeated manner (Hertweck, 1931; Crossley, 1978; Bate, 1990). The peripheral nervous system (PNS) innervating these muscles also follows a segmentally repeated pattern, with no apparent differences between abdominal segments A2 through A7 throughout the embryonic stages (Fig. 1).

Each of the abdominal MFs is innervated by a consistent set of axons, which form junctions with shapes and locations specific to a given fiber. These have been divided by morphological criteria into Type I junctions, with one or more linear chains of relatively

←

long filopodia, including some (*arrowheads*) that originate below the point at which the junctions typically form on MFs 1 and 9. The long filopodium at the lower right of the ISN belongs to a growth cone on MF 2, the remainder of which is out of view. *B*, The junctional aggregates appear structurally more complex (14.5 hr AEL). Portions of the growth cones innervating MFs 1 and 9 are spreading to both the internal and external surfaces of MF 1, as indicated by the two very different planes that can be seen in the stereo pair. Regional thickenings or portions that are more heavily labeled can be distinguished, seeming to condense from the more evenly labeled growth cone of earlier stages. *C*, Branches or divisions of the growth cones (16 hr AEL) are extending both over the internal surface of MF 1 and along its external surface in the cleft between MF 1 and MF 9 (which lies more lateral to MF 1). The divisions of the junctions that typically extend from the NEP both anteriorly and posteriorly on MF 1 appear to be forming (*arrowheads*). The junctional aggregate of MF 9 typically spreads posteriorly from the ISN. *D*, The distinction between the junctional aggregates of MFs 1 and 9 is now discernible because of the increase in length of the connecting portion of the ISN (16.5 hr AEL). A small cylindrical thickening is visible in a posterior branch on MF 1 (*arrow*). Overall, the impression at this stage is that the planar growth cone is condensing to form thicker, branch-like structures, but numerous filopodia are still present. *E*, There are three separate regions (*arrowheads*) in which terminals have formed noticeably thicker, three-dimensional structures (17 hr AEL). Only the surface membrane is labeled, so the impression of hollow structures is given. On the anterior (*left*) growth cone on MF 1, the stereo pair shows what could either be a large flattened structure or two separate thinner structures lying on top of each other. Electron microscopic observations of this stage indicate that both interpretations are possible. We refer to the single enlarged regions of a terminal as prevaricosities. *F, G*, By 19 hr AEL (*F*), and continuing through hatching (*G*), the enlarged structures along terminal branches began to have more clear-cut constrictions on either side of them. Their shapes ranged from tubular to spherical. We view this process as giving rise to the first real varicosities of the developing terminal. The dimensions of the individual spherical structures were typically less than those of the prevaricosities. Multiple terminal branches appear to be present. The *arrowheads* in each panel point to much thinner terminal branches, which are superimposed on the larger varicosities; these could be either Type Is or II, if, as might be expected, the largest varicosities are from Ib terminals. Filopodia are still present but tend to be somewhat fewer in number and shorter relative to the dimensions of the enlarged thicker regions. This transition is diagrammed in Figure 7*C,D*.

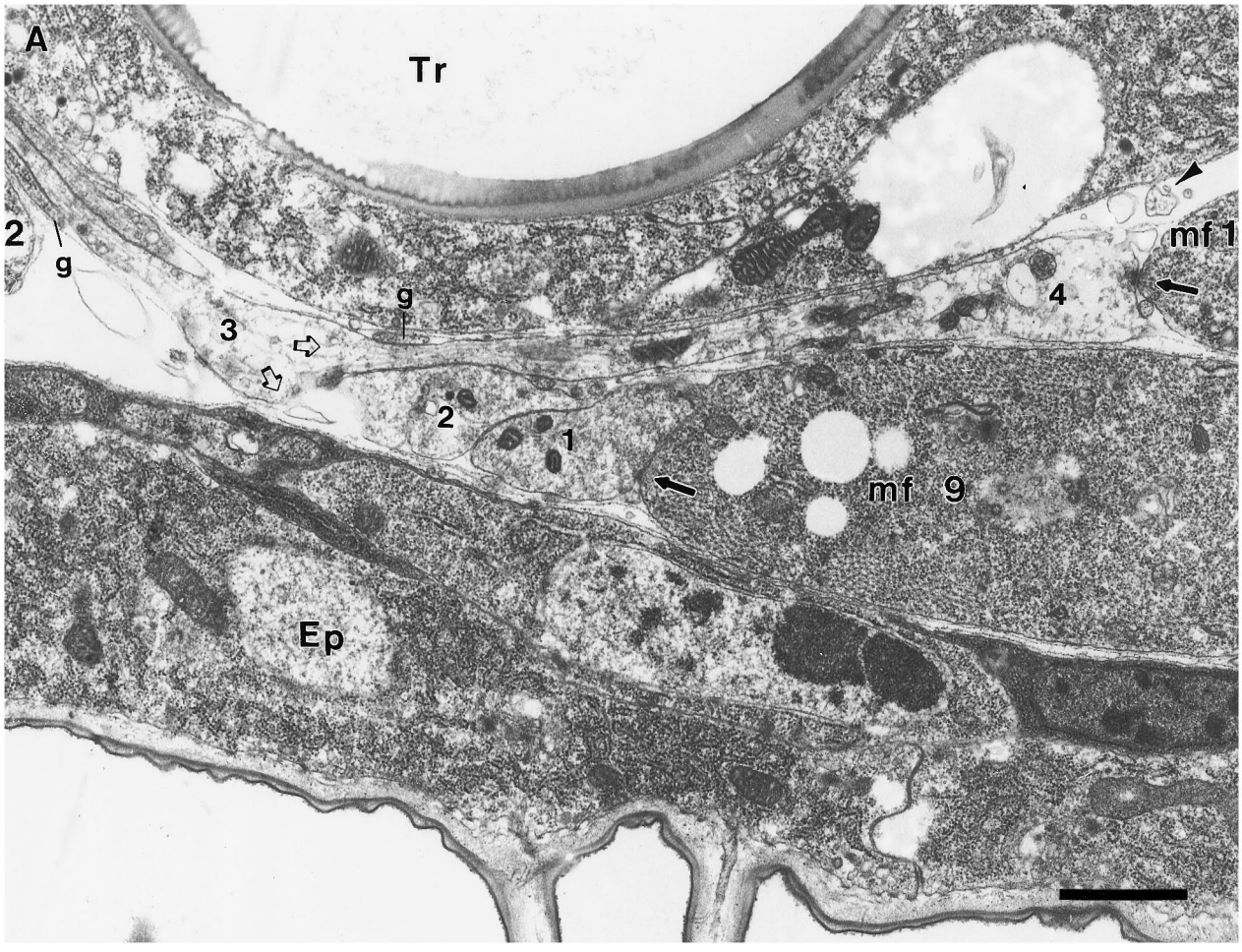

Figure 6. Junctional aggregates of MFs 1 and 9 at the prevaricosity stage (17 hr AEL). The animal was not filleted but fixed by perfusion through the tail end, so the nerves and muscles are lying in their natural positions. *A, B*, and *C* are sections 12, 32, and 52, respectively, from a series. *Ep*, Epidermal cell; *Tr*, main dorsal tracheole; *g*, parts of glial process on the distal part of ISN. *A*, This section passes through the center of the NEP for MF 9 (*mf 9*) and just off center for the NEP on MF 1 (*mf 1*). Notice the swellings in the axonal profiles at the NEPs compared with their diameter at the dorsal edge of MF 2, at the *left* of the micrograph. These enlarged profiles can be compared with the prevaricosities shown in Figures 1, 3, and 4. Three overlapping axonal branches are found in the NEP of MF 9 in this plane of section. Axon 3 (numbers applied solely for identification in this animal) is bifurcating at this point (*open arrows*), with one branch following the axons that are headed toward MF 1 and one branch continuing eventually to the surface of MF 9. Elementary synapses are seen at the contact points of axons 1 and 4 with their respective muscles (*arrows*). A profile of a filopodium from a growth cone lying more dorsally (out of the field of view) next to MF 1 is indicated with an *arrowhead*. One edge of the glial covering of the ISN is indicated (*g*), but the axons and terminals in this region are largely naked. At higher magnification it can be determined that the nerve passing over MF 9 en route to MF 1 actually consists of several axonal branches cut very obliquely. Scale bar, 1 μm. *B*, NEP on MF 9, anterior to 6A. Axon 1 has formed a synapse with MF 9 (*arrow*), and axon 2 has formed a dense body in apposition to axon 1 (*open arrow*). Axon 2 branches on both sides of another axonal profile. Note the difference in synaptic vesicle size between axon 1 and axon 2. Scale bar, 0.5 μm. *C*, Anterior edge of NEP on MF 9. Axon 1 remains in contact with MF 9; the other axonal branches have turned laterally and are now seen in cross section (*asterisks*). Compare with Figure 5 to visualize. Focal contacts and elementary synapses are formed by axon 1 with MF 9 (*arrows*). Scale bar, 0.5 μm. *Figure continues.*

large varicosities, a distinctive subsynaptic reticulum (set of highly convoluted folds) formed by the MF around the terminal, and muscle-specific branching patterns, and Type II junctions, with long trailing branches composed of very small varicosities, and which lack a subsynaptic reticulum (Johansen et al., 1989a; Atwood et al., 1993; Jia et al., 1993). The Type I junctions, where they have been investigated, are thought to use glutamate as a primary neurotransmitter (Jan and Jan, 1976; Johansen et al., 1989a). The Type II junctions include octopamine, and all the terminals of this type in one hemisegment are derived from branches of only two neurons (Monastirioti et al., 1995). A third general type, Type III, includes terminals with peptidergic transmitters, one example of which is immunoreactive for an insulin-like peptide and is known only to innervate MF 12 in segments 2–5, and has more oval-shaped boutons than Type II terminals (Gorczyka et al., 1993).

Certain of these MFs have been studied more extensively than others. In particular, the very large MFs 6 and 7 (nomenclature after Crossley, 1978; Bate, 1990) are usually innervated only by two Type I terminals, which have been subdivided into Ib and Is on the basis of morphological criteria (Ib boutons are larger) and functional differences (Ib terminals produce smaller excitatory junction potentials) (Atwood et al., 1993; Kurdyak et al., 1994). These two terminal types are thought to be derived from two separate neurons: RP3 and 6/7b (Sink and Whitington, 1991; Keshishian et al., 1993).

We examined the normal development of the nerve terminals innervating the dorsal longitudinal fibers 1 and 9 and compared

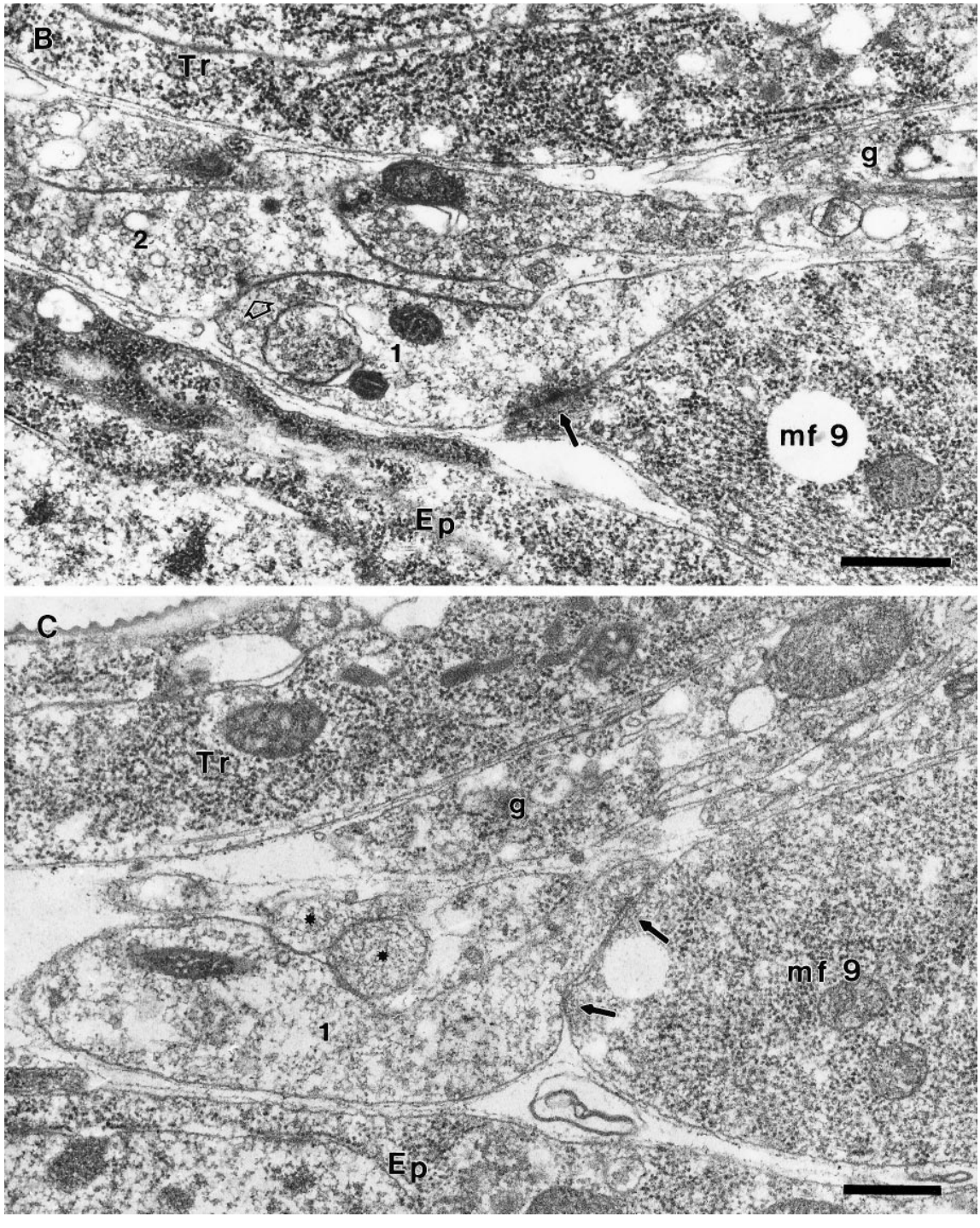

Figure 6 continued.

the results with those we obtained concurrently from MFs 6 and 7 in segments A2–A7, as well as with those described previously for MFs 6 and 7 (Broadie and Bate, 1993). The terminals on MFs 1 and 9 are conveniently accessed in the embryo for electrophysiological studies. Their terminals, unlike those of MFs 6 and 7, are well spread in the *x-y* plane and easy to observe in structural studies (Fig. 1*A*). MFs 1 and 9 have two types of terminals, with relatively large boutons that seem to correspond structurally to Types Ib and Is as described for MFs 6 and 7, as well as Type II terminals, (Fig. 2, *A* and *C*, for MFs 1 and 9, *B* and *D* for MFs 6 and 7), a pattern that is characteristic of most of the other abdominal segment fibers. In this study we have emphasized the latter part of embryological development to provide a solid baseline for future studies of mutants with defects in their neuromuscular junctions, and that, therefore, would be less able to survive past hatching.

Mature innervation of MFs 1 and 9

The terminals innervating MFs 1 and 9 are the most dorsal in each segment and are at the distal end of the ISN. Their supply-

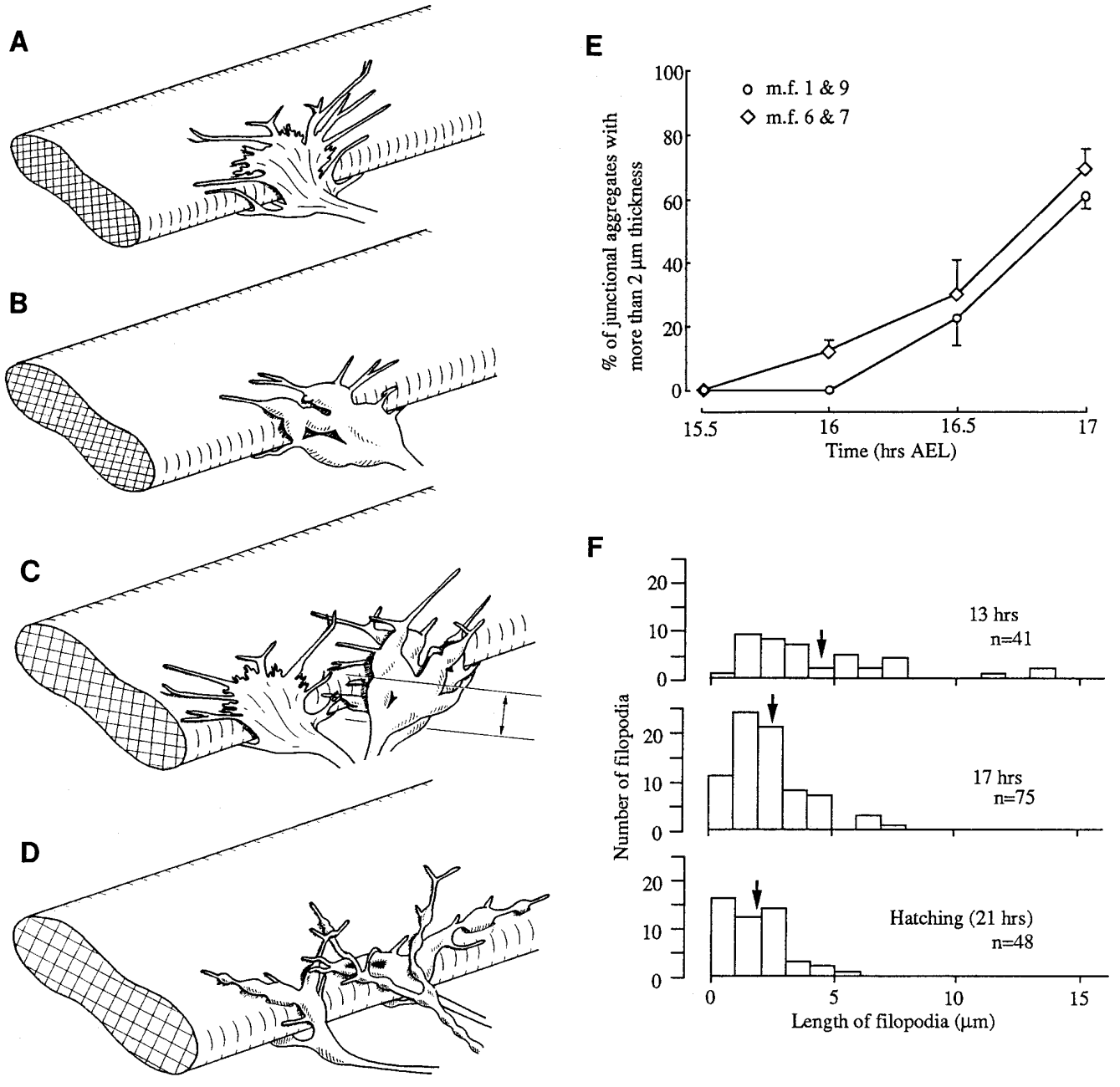

Figure 7. *A–D*, Diagrammatic representation of steps in development of the junctional aggregate on a single MF. *A*, Growth cone stage. During the growth cone stage, the developing terminal is thin and flat, with long filopodia. The growth cone from a single axon is illustrated. However, it often appears that toward the end of the growth cone stage two or more growth cones are overlapping in the vicinity of the NEP. *B*, Prevaricosity stage. The prevaricosities formed by a single axon are shown for simplicity. The growth cone condenses into several recognizable branches that have distinct thickness and rounded contours. Filopodia are shorter. Simple presynaptic specializations form along broad contact regions with the MF. *C*, Junctional aggregate at the prevaricosity stage, ~16.5–18.5 hr AEL. During the prevaricosity stage, several terminals of differing degrees of development are usually found overlapping at the NEP. In this example, a growth cone is shown slightly diverging to the *left*, and two overlapping terminals with prevaricosities are to the *right*. Many additional configurations have been observed. When terminals have entered at the same point, they often remain spatially close, with membrane-to-membrane contact for some distance away from the NEP. This leads to a very complicated appearance when seen at either the light microscope or SEM levels. The *bracket* indicates the regions that were measured to quantify prevaricosity formation in *E*. *D*, At 18–19 hr AEL, distinct varicosities, swellings with constrictions on either side, resolve from the enlarged branches of the prevaricosity. A single swelling may divide itself into two or three discrete varicosities. Filopodia are shorter, the elements of the SSR begin to separate the broad nerve–muscle contact regions, and individual bouton types can begin to be recognized. Subsequent development between this stage and first instar is a matter of degree of development of individual varicosities. *E*, Time course of prevaricosity formation. The percentage of junctions having prevaricosities and/or layered structures with a total thickness >2 μm was determined for each stage for MFs 1 and 9 (*m.f. 1 & 9*) and for MFs 6 and 7 (*m.f. 6 & 7*). The dimension of 2 μm was an arbitrary criterion to mark prevaricosity formation, with some individual prevaricosities being larger and some being smaller than this size. By 17 hr AEL nearly all junctions on MFs 1 and 9 included prevaricosities by subjective criteria, but not all reached the 2 μm thickness criterion. Subjectively, in a given animal or at a given age, the swelling of the prevaricosity seemed to be greater in the more ventral muscles than in the more dorsal ones (Figs. 1, 4, 11). To quantify this difference, the 2 μm criterion was applied to MFs 6 and 7 in the same animals. There appears to be a delay of ~15–30 min in the initiation of the process from dorsal to ventral muscles. For MFs 1 and 9, the total number of junctions measured at 15.5 hr AFL was (*Figure legend continues*)

ing nerve trunks are therefore not complicated by either axon tracts innervating other muscles or ingrowth of sensory axons (Campos-Ortega and Hartenstein, 1985). One of the neurons innervating MF 1 is the aCC neuron (Sink and Whitington, 1991; Van Vactor et al., 1993), but the others innervating MFs 1 and 9 have not yet been identified. Anti-HRP labeled preparations, both at the light microscope level and with SEM (Fig. 3), show that one of the large axons consistently bifurcates at the dorsal edge of MF 2 (Fig. 3, *thin arrow*), sending one branch to MF 1 and one to MF 9. Perhaps this shared innervation is derived from one of the U neurons, analogous to the U neuron innervating both MF 2 and MF 10 (Sink and Whitington, 1991). A small-diameter axon is also seen to bifurcate at the same level; this axon formed varicosities within the nerve trunk as well as on the MFs themselves, similar to the pattern illustrated for the two octopaminergic neurons per hemisegment that provide Type II innervation to many of the fibers in the body wall (Monastirioti et al., 1995). Two large-diameter axons consistently proceed separately to MF 1 and MF 9. Sections through the ISN over the center of MF 2, before this bifurcation point, typically show the presence of four axons. This working hypothesis of the innervation pattern of MFs 1 and 9 is illustrated in Figure 1*C*. It remains to be confirmed by single cell injections or other more specific methods.

We refer to the cluster of different terminals on each fiber, two of which may be excitatory, as in MFs 6 and 7, and one or more of which may have neuromodulatory properties, as a "junctional aggregate," to distinguish the case from the situation in vertebrates in which one motor neuron forms a single neuromuscular junction per MF. Most insects have muscles that are multiterminally innervated, with evenly spaced terminals all along each fiber, as well as muscles that are multineuronally innervated (Hoyle, 1955; Usherwood, 1974; Rheuben and Reese, 1978; Schaner and Rheuben, 1985), but the single cluster of large junctions found on *Drosophila* larval muscles is relatively unusual, presumably arising from the electrically very short MFs, which make multiterminal endings unnecessary. The point at which the nerve branch first contacts the MFs is described as the NEP.

Development of the terminals innervating MFs 1 and 9

The development of the synaptic terminals innervating MFs 1 and 9 was examined using both ultrastructural and confocal light microscopic methods. The antibody to horseradish peroxidase, anti-HRP, which recognizes a carbohydrate with which several glycoproteins in the membranes of insect neurons are decorated (Snow et al., 1987; Katz et al., 1988), was used to demonstrate the embryonic axons and terminals more clearly, and an antibody to synaptotagmin was used as a monitor of intracellular synaptic development. Confocal microscopy with fluorescent-labeled primary or secondary antibodies and stereo pairs made it possible to study the spatial distribution of terminals and allowed terminals on both sides of an MF to be visualized. Furthermore, one could make the large number of preparations needed to assess developmental time courses using this method. Scanning electron microscopy provided high magnification overviews of the terminals and allowed us to visualize the structures that the terminals were in contact with. Thin sections provided identification and clarification of the subcellular characteristics of these developing terminals.

Growth cone stage

In a series of timed embryos whose PNSs were observed with fluorescein-labeled anti-HRP and confocal microscopy, we found that one or more of the growth cones of the ISN consistently reached the vicinity of MFs 1 and 9 by ~13 hr AEL, as described previously (Johansen et al., 1989b; Sink and Whitington, 1991; Van Vactor et al., 1993).

At 13 hr AEL, at least one growth cone extended numerous long filopodia over much of the surfaces of each of these dorsal MFs, including regions in which junctions were not expected to form (Fig. 4*A*). Subsequently, the middle planar region of the growth cone expanded on the surface of its target MF, largely over the future junctional site, and the origins of filopodia were more restricted to this region (Fig. 4*B*). In some cases the growth cones and filopodia appeared to be adhering primarily to the internal surfaces of both MF 1 and MF 9. In other cases, parts of growth cones also invaded the cleft formed by the external surface of MF 1 (dorsolateral in the living embryo) and the internal surface of MF 9 (Fig. 4*B*). This fits with observations on mature larvae in which some terminal branches on MF 1 reach around to the external side, whereas the rest lie on the internal surface. Although the MFs themselves are not visible in the images formed with fluoroscein-labeled anti-HRP, they could be seen concurrently with differential interference contrast optics; they are indicated schematically on the figures by gray lines. The different growth cone locations can be seen by using the three-dimensional imaging provided by the stereo pairs.

This period, in which the middle region of the growth cone was flat and the filopodia were long, lasted for ~3.5 hr. The form of the growth cones appeared to be as labile as that observed previously in the segmental nerve with time lapse photography (Keshishian et al., 1993), in which filopodial extensions and retractions of 15 μm occur over a matter of minutes. Although transmitter release has been shown to occur during this period (Broadie and Bate, 1993; Nishikawa and Kidokoro, 1995), presumably few permanent morphological release sites have formed because of the labile structure. There was little overall change in characteristic structure at the light microscope level during this time, and we refer to this period as the "growth cone period."

Toward the end of the growth cone stage, strand-like structures were seen in conjunction with some of the broad, sheet-like lamellipodia, and there was an impression of greater complexity in both confocal and SEM images (Figs. 1*A*, 4*C*). This apparent complexity could arise either from the superimposition of the lamellipodia of one growth cone over the filopodia of a second, or from multiple branches of the same growth cone. Because most earlier studies were made by either injecting the cell body of the aCC neuron (Sink and Whitington, 1991) or labeling all of the axons and growth cones with anti-HRP, as we have done, the presence of the growth cones of other axons innervating MFs 1 and 9 has not yet been determined.

←

n = 23 (4 animals); 16.0 hr, n = 42 (8 animals); 16.5 hr, n = 56 (10 animals); 17.0 hr, n = 46 (6 animals). MFs 6 and 7, at 15.5 hr AEL, n = 22; 16 hr, n = 46; 16.5 hr, n = 56; 17 hr, n = 36, respectively, for the same animals. The fraction of terminals reaching prevaricosity stage was tabulated for each animal; the points plotted represent the mean of these values ± SEM. *F*, Decrease in filopodial length with increasing age. The lengths of filopodia of the terminals innervating MFs 1 and 9 were measured from projected images along the *z* axis for three terminals at each age. At 13–14.5 hr AEL, some very long filopodia, >10 μm, are present; by hatching, all the filopodia are <6 μm. The *arrows* indicate the average filopodial length at each stage.

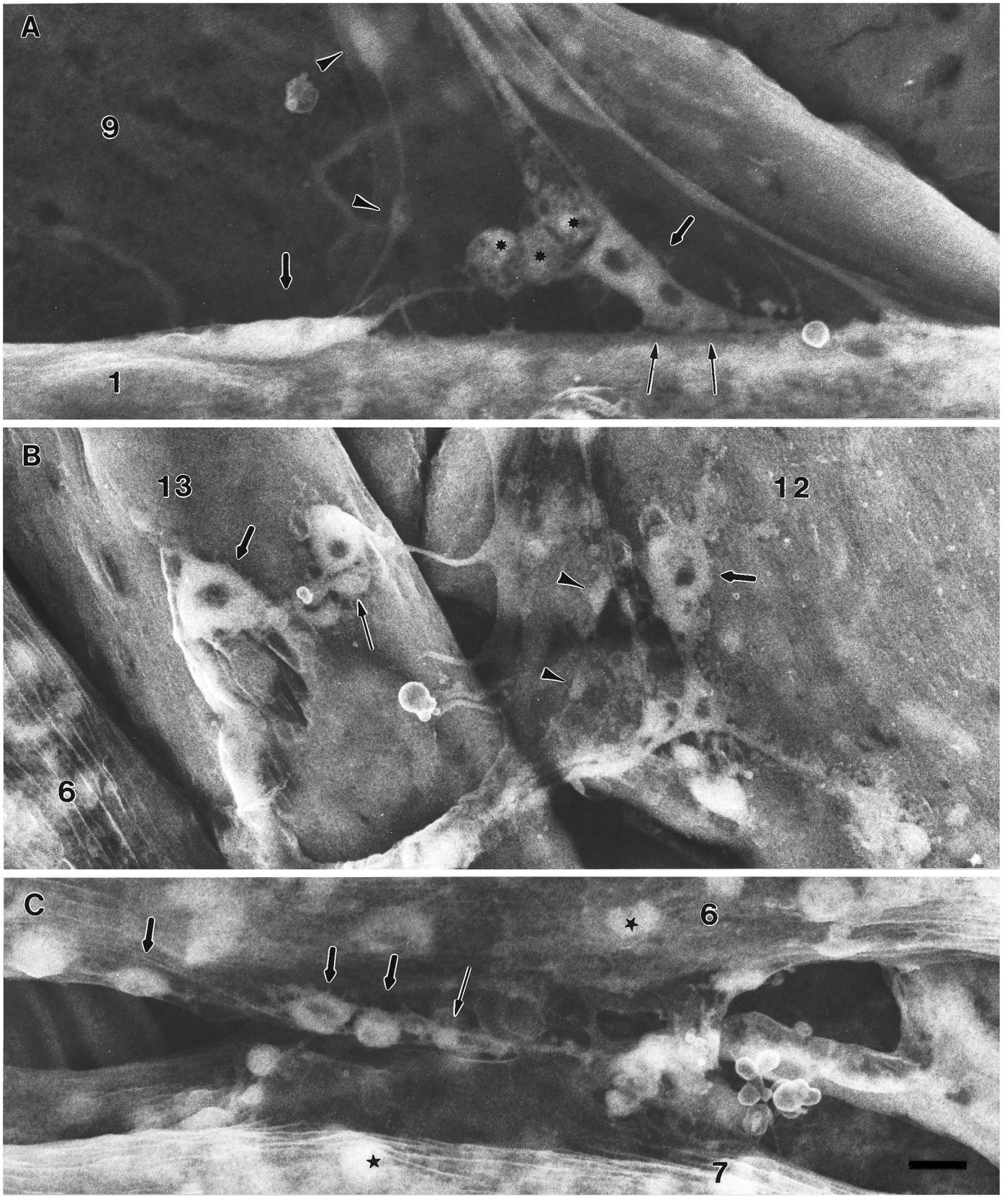

Figure 8. Junctional aggregates at the varicosity forming stage, 19 hr AEL, from three sets of muscles of the same abdominal segment. The varicosities are less well defined in MFs *1* and *9* (*A*) than in the ventral muscles *12* and *13* (*B*) or *6* and *7* (*C*). These SEM specimens were prepared only with OTO. Accelerating voltage, 10 kV. Scale bar, 1 μm for all. *A*, The transition from the prevaricosity to constricted varicosities is evident in two terminal branches on MF 1. Two angular elongated shapes (*thick arrows*) appear to be in the process of each being subdivided into two varicosities. The developing varicosities contain "hollow" regions similar to those seen in larval junctions. (Dark appearance implies absence of (*Figure legend continues)*

We examined a series of embryos for evidence that the multiple innervation of MFs 1 and 9 was present by the late embryo stage. In thin sections, at 15.25 hr AEL, growth cone-like nerve structures (vacuolated unspecialized cytoplasm, ruffled profiles) were found over many of the body wall muscles in rather loose associations. At the NEP, two or three slightly enlarged axonal profiles were superimposed. Distinguishing cytoplasmic specializations were lacking, and processes spreading away from this point were not tightly adherent to the muscle.

By 16 hr AEL, serial thin sections of the ISN over MF 2 showed four axons that would all be destined for MFs 1 and 9 at that point. This would represent the full complement of the innervation for the two muscles if none were secondary branches. In embryos older than 15 hr AEL, most body wall muscles, including MFs 1 and 9, were contacted by two or more axons, and these axon terminals were structurally distinguishable from each other by 16–17 hr AEL. Adjacent terminals on the same MF differed in vesicle type and cytoplasmic inclusions and were derived from separate axonal branches. Terminals with the vesicle composition and morphology of Type I axons were present, as well as those containing irregularly shaped dense-cored vesicles characteristic of Type II terminals. Consequently, we conclude that by the end of the growth cone period, multiple and possibly all axons are represented in the junctional aggregate as growth cones or as developing terminal structures.

Prevaricosity stage

At 16.5 hr AEL, the axons and planar central regions of the growth cones suddenly began to enlarge and increase in thickness at the site of the future NEP for each MF (Figs. 1*A*, 3, 4*D*). These enlarged regions reached up to 5 μm in length and 1–3 μm in thickness and might be subdivided into two or more "hollow-appearing" structures. The hollow appearance arises from the use of a labeling antibody that is recognizing membrane-bound antigens, leaving the center of the terminal unstained. We refer to the enlarged structures as "prevaricosities." Their shapes were as variable as those of the growth cones. Some were long and ellipsoid, whereas others were tubular or polygonal with distinct angles (Figs. 3, 4*D*, 12*B*). Overall their outline and position seemed to reflect that of the original growth cones before the thickening occurred. By 17 hr AEL, almost all terminals had one or more prevaricosities, and several might be grouped at the NEP to form a quite thick structure (Fig. 4*E*). Sometimes an apparent ventral-to-dorsal gradient in degree of development could be recognized within a single abdominal segment (Fig. 1) (see comparison with MFs 6 and 7 described below).

SEM images of the junctional aggregates from animals 16–18.5 hr AEL also showed a complicated structure, with layered intertwined processes radiating outward from the NEP (Fig. 5). Evidently part of the increase in thickness in the confocal images was attributable to axonal processes lying one on top of another. In addition, individual processes often had an enlarged region (~1 μm in cross section) at the NEP, and which then divided into smoothly tapered small diameter branches (0.2 μm) that continued across the surface of the fiber (Figs. 1, 3). The enlarged regions seemed to correspond to the prevaricosities seen confocally and described in the previous paragraph, and the small-diameter branches seemed to be residual filopodia.

To elucidate this complicated structure, serial sections were taken through parts of the NEPs and junctional aggregates of MFs 1 and 9 from two embryos within the prevaricosity period. Sections from the oldest, 17 hr AEL are illustrated in Figure 6*A–C*. The following features were seen in both animals. (1) Two or more axons formed enlarged bulbous regions as they approached the NEP of each MF. These axons could be distinguished from each other throughout the series on the basis of their cytoplasmic inclusions and type of vesicles, but they could not always be assigned to a particular mature type such as Is or Ib (Fig. 6*A*). (2) At the NEPs of both MF 1 and MF 9, one of the enlarged axons typically formed a broad uninterrupted contact with the MF. This contact region housed 10 or more immature synaptic specializations. The vesicle type and dense body structure were consistent with its being a Type I terminal. (3) The enlarged region of the second axon, which had larger and more irregularly shaped clear-cored vesicles as well as dense-cored vesicles, (Type II?) typically lay on top of the first axon at the NEP. Four examples were encountered in which it formed a synapse-like structure in apposition to the first axon (Fig. 6*B*). This second axon was not seen to form synapses in apposition to the MF within the available sample of sections. (4) At the NEP of MF 9, a third axon was typically found outside the second. It bifurcated and one branch was directed toward MF 1, whereas a second was traced to the surface of MF 9. It appeared to be from the other Type I axon. (5) Processes with the morphological characteristics of growth cones were also seen in the vicinity of MFs 1 and 9 at this time. They were not successfully traced to a specific parent axon, so their origin is uncertain.

We conclude that axons with phenotypically differentiated characteristics are forming terminals by the prevaricosity stage. Their swelling and superimposition results in the dramatic increase in thickness of the junctional aggregate seen at this time. The transition from the growth cone stage to the prevaricosity is presented diagrammatically in Figure 7*A–D*.

To assess the time course of prevaricosity formation, the thickness of the overall structure was assessed using *z*-axis measurements of the confocal images. The growth cone was essentially a planar structure, whereas >60% of the prevaricosities, or the joint structures formed by layers of prevaricosities, growth cones, and filopodia, had a thickness >2 μm measured in the vicinity of the NEP. Using this dimension as an arbitrary cutoff point between the growth cone stage and the prevaricosity stage, we counted the number of segments that had terminals or layers of terminals >2 μm in thickness at the NEP of MFs 1 and 9, from 15 to 17 hr AEL (Fig. 7*E*). The abrupt increase in the numbers of thick structures from 16 to 17 hr AEL is evident.

←

osmiophilic structures such as organelles or synaptic vesicles.) In addition to major divisions, each terminal branch of an apparent Type Ib axon continues to extend thin filopodial or sprout-like processes to the MF. The strong adhesive nature of the nerve–muscle contacts (*thin arrows*) is evident because of the tension placed on the ISN. Type II axons form varicosities within the nerve by this time (*arrowheads*). The third axon, presumably Is, forms branches on the lateral side of the MF that are not seen here. Spherical, granular-appearing cells, which may be the persistent *twist* cells (*asterisks*), are often seen at the NEP of MF 1. *B*, On MFs *12* and *13* it is possible to recognize several different terminal types by 19 hr AEL. Two or three large Type Ib varicosities are found on each fiber (*thick arrows*) as well as varicosities of other types (*thin arrow* and *arrowheads*). *C*, On MFs *6* and *7*, large and small varicosities (*thick* and *thin arrows*) have formed in the region of adherence between the two fibers. Other approximately spherical structures (*stars*) within the MF can be distinguished from varicosities on the basis of their focal plane and absence of connecting neurites.

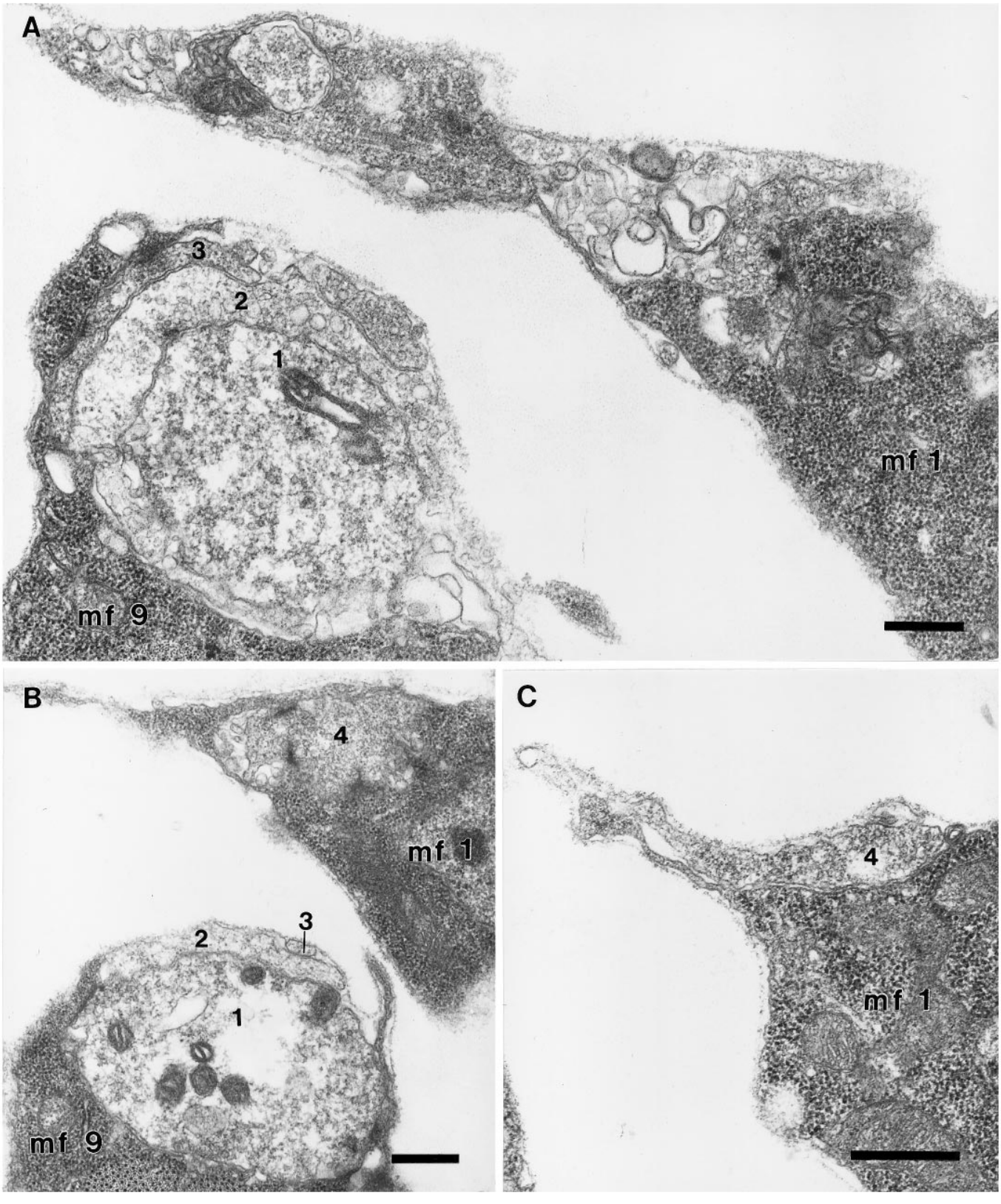

Figure 9. Junctional aggregates on MFs 1 and 9 at 19 hr AEL. *A, B, C*, Serial sections 231, 242, and 254, respectively. The embryo was dissected flat for fixation, so the tension on the ISN has pulled the NEP on MF 1 toward MF 2. Scale bars, 0.5 μm. *A*, On MF 9 (*mf 9*), axon 1 has formed a spherical varicosity that is almost completely wrapped by two other terminals (*2, 3*). In this plane of section, axon 2 has formed a synapse in apposition to axon 1, and axon 3 has formed electron-dense specializations in apposition to a thin arm of the MF. The vesicle sizes in axon 1 were more uniform and smaller than those seen in axon 2. Axon 2 had numerous dense-cored vesicles elsewhere in the series. A growth cone was part of the aggregate in another plane (not shown). At this level, numerous small tangled profiles were seen on MF 1; they included branches from axon 2 just seen on MF 9, and from a growth cone-like structure as well as an axon that formed Type I varicosities in apposition to the MF. *B*, Axon 1 on MF 9 (*mf 9*) (*Figure legend continues*)

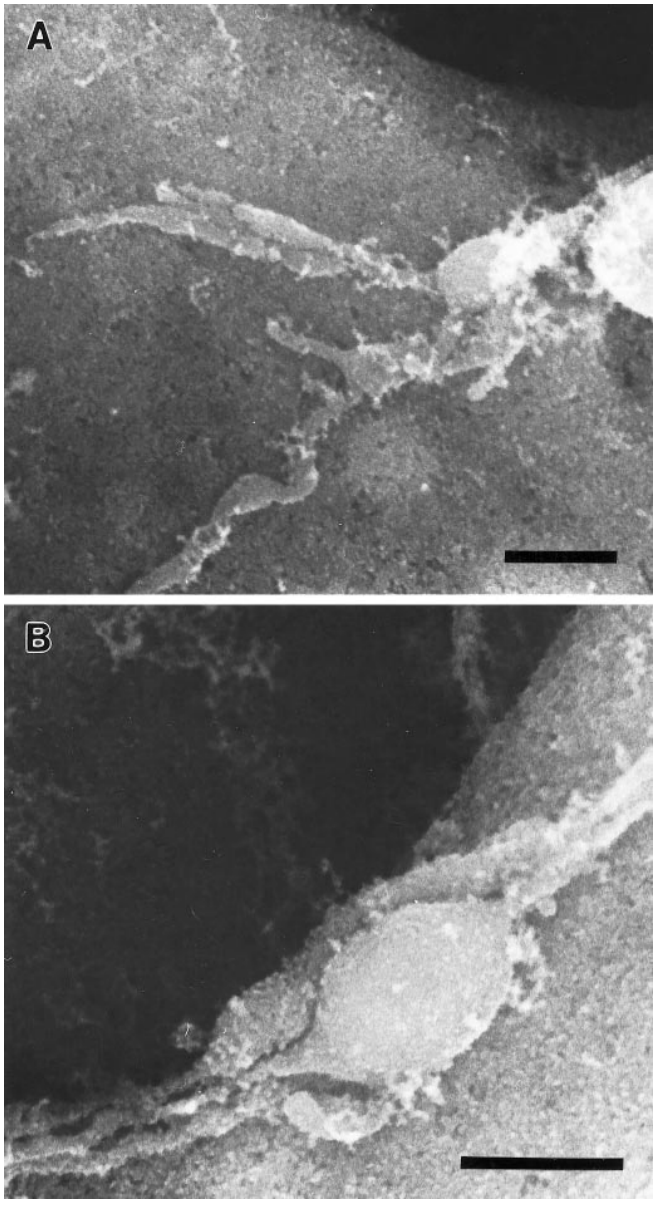

Figure 10. Varicosity formation, MF 9. At 19 hr AEL, the more distal regions (*A*) of nerve terminals have irregular sprout-like shapes; varicosities are formed in the neurites closest to the NEP (*B*). In both regions the processes from one or more different axons are typically intimately intertwined, with membrane-to-membrane contact (verified by TEM views; see Fig. 9*A,B*), which is maintained over long distances as seen here. This is different from the mature larval form in which Types Ib and Is are at least separated from each other by layers of subsynaptic reticulum. The basal lamina was removed by treatment with 25% KOH for 2 min at 60°C after fixation, followed by osmium-thiocarbohydrazide. Scale bars, 0.5 μm.

Varicosity stage

After 17 hr AEL, another structural transition was observed. The large prevaricosities began to appear constricted into several smaller swollen regions. By 19 hr AEL, some of these constricted regions had the spherical appearance of the individual varicosities or boutons as seen in first instar and older larvae. (Hatching occurred at 21 hr AEL at 25°C under these culture conditions.) Between 19 hr AEL and hatching, some of the enlarged structures developed a series of dark-appearing central regions in SEM, reflecting an absence of osmiophilic structures in the centers of the terminals (Fig. 8). Others continued to look like tubes separated by constrictions, or they formed other irregular shapes. The size of a single large approximately ovoid varicosity, derived from a prevaricosity near the NEP, was ~2 μm in width and 3–4 μm in length, which is within the range of the Type I boutons in third instar larvae (Atwood et al., 1993). Subjectively, there again appeared to be a small ventral-to-dorsal gradient in the development times of the varicosities (Fig. 8), but this was not quantified.

The NEP retained a complex form during the varicosity stage. Multiple layers of axon and terminal branches were still superimposed (Fig. 9). Most of the long filopodia have been retracted by this time, but shorter filopodia, sprouts, and side branches continued to arise from both the varicosities and the neurites between varicosities (Figs. 4*F*, 8). The average lengths of filopodia gradually decreased (Fig. 7*F*). At 13 hr AEL, some terminals had filopodia >10 μm in length, and there was a great variation in their lengths. In later stages, the distribution of lengths shifted to an average of <5 μm. From 19 hr AEL through hatching, slender filopodia-like structures were still present in the distal parts of the terminals (Figs. 4*F*, G, 10*A*). With confocal or SEM microscopy on fixed tissue, it is not possible to determine whether these should be considered functionally as filopodia or neurites. They presumably remain to add new varicosities as growth of the MF continues. Commonly two or more terminal branches, including those having varicosities, remained intimately intertwined for some distance as they crossed the surface of the MF (Fig. 10*B* and TEM sections not illustrated). This configuration differs from that illustrated for third instar larvae (Atwood et al., 1993; Jia et al., 1993), in which terminals are separated from each other by a region of subsynaptic reticulum at the very least. Some very slender "stick-like" terminal structures were seen along with the varicosities forming after 19 hr (Fig. 4*F*). These lacked obvious varicosities and may be the early form of Type II terminals. In TEM, Type II terminals were clearly identified by their vesicle composition and morphology on MFs 1 and 9 by 16 hr AEL.

Development of the terminals innervating MFs 6 and 7

We compared the developmental time course of the terminals innervating MFs 6 and 7 with that observed for MFs 1 and 9, looking for both quantitative differences that might arise from the greater distance that the ISN axons have to grow or qualitative differences that might arise from properties of the different axons that innervate these muscles. The terminals on MFs 6 and 7 developed in a manner similar to those of MFs 1 and 9 (Fig. 11). During the early stages, the growth cone or growth cones spread along the cleft between the two fibers (Fig. 11*A*), where they formed a planar structure that was generally perpendicular to the plane being viewed, and which was often directly superimposed

←

formed a total of eight presynaptic active zones of the multi-branched type in apposition with the MF in this and subsequent sections through this varicosity (0.7 × 1.0 × 1.7 μm), and three more in a second smaller one. The varicosity (axon 4) shown on MF 1 (*mf 1*) was 1.7 × 1.0 × 1.1 μm and housed six active zones; in this grazing section their multipronged nature can be seen. *C*, At the edge of the NEP, a single relatively unspecialized profile of axon 4 continues across the surface of MF 1.

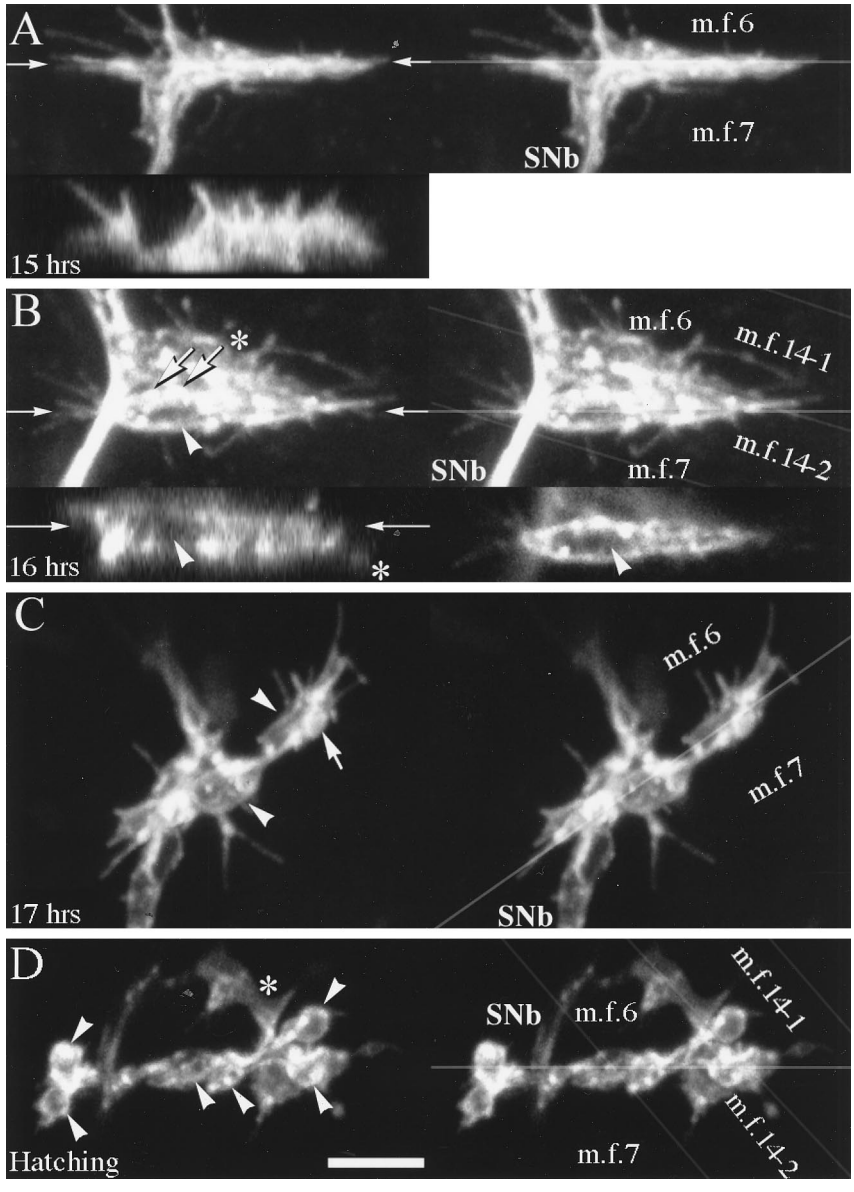

Figure 11. Prevaricosity formation was compared in the terminals innervating MFs 6 and 7. *A*, At 15 hr AEL, the stereo pair illustrates growth cone lamellae and filopodia, which are spreading both upward over the surface of MF 6 (*m.f.6*) as well as along the cleft between MFs 6 and 7 (*m.f.7*). In the cleft, part of the junction appears as a vertical plate-like structure, with subdivisions that extend directly into and out of the plane of optical section. In the *x-z* image (*bottom left* in *A*), the upwardly directed filopodia and the vertical extent of the growth cone are illustrated. The location of the *x-z* section, in the center of the cleft between MFs 6 and 7, is indicated by the *pair* of *arrows*. It is not possible in the confocal images to determine whether apparent subdivisions of the growth cone are derived from different axons. *B*, Beginning of prevaricosity formation (16 hr AEL). In this stereo pair the image of the innervation of MFs 6 and 7 is superimposed on that of subsequent branches of SNb (*asterisks*) that innervate MFs 14–1 (*m.f.14–1*) and 14–2 (*m.f.14–2*) (Bate, 1990). A tubular prevaricosity belonging to MFs 6 and 7 is indicated by an *arrowhead*. The cylindrical nature of the prevaricosity is shown more clearly in a single *x-z* section, *bottom left* (*B*), and an *x-y* section, *bottom right* (*B*), (*arrowheads*). Thinner terminals with small varicose regions (*thick arrows*) may lie on top of this prevaricosity; in addition, however, small "spots" of increased fluorescence are seen where small processes emerge from the prevaricosity perpendicular to the plane of optical section. The *pairs* of *thin arrows* indicate the planes of section of the *x-z* and *x-y* images. *C*, In this junctional aggregate on MFs 6 and 7 (17 hr AEL), two large prevaricosities are seen (*arrowheads*). Additional thinner terminal branches with small swellings (*arrow*) also appear to be present and are closely intertwined with the prevaricosities. It is possible that these are terminal branches from the second axon, which is known to be present at this time from physiological findings (Broadie and Bate, 1993). Note, however, that the bases of filopodia also give rise to small dots of increased fluorescence, which at first glance may appear to be small varicosities (*above lower arrowhead*). *D*, *Hatching*, 21 hr AEL. Six large varicosities are present in the cleft between MFs 6 and 7 (*arrowheads*), as well as some smaller ones. Note that the varicosities are smaller than the enlarged swellings shown in *C*. *Asterisk* indicates the 14–1, 14–2 junctions. The stereo pairs are helpful to exclude their varicosities from any counts of the varicosities of the 6–7 junction. Scale bar (shown in *D*): 5 μm for all panels.

on the terminals innervating MFs 14–1 and 14–2. Subsequently, portions of the growth cones swelled to form prevaricosities (Fig. 11*B,C*). After this period, the prevaricosities were constricted to form a series of more typical varicosities (Fig. 11*D*). Overall, these processes appeared to be quite similar to those observed on MFs 1 and 9.

The time course of development for MFs 6 and 7, however, seemed to be slightly earlier than for MFs 1 and 9. This was observed subjectively in segments in which MFs 6 and 7 had already formed several distinct varicosities or prevaricosities, whereas the dorsal muscles in the same segment had not reached the comparable stage (Fig. 8). Objectively, prevaricosity formation was detectable in MFs 6 and 7 at 16 hr AEL, using the minimum dimension of 2 μm in thickness (width in the *x-y* plane) as a criterion (Fig. 7*E*). This was about 0.5 hr earlier than for MFs 1 and 9.

The time of varicosity or bouton formation that we are reporting is later than that reported by Broadie and Bate (1993a), but this relates partly to differences in the application of the term "bouton" to enlargements of the developing terminal. In addition, we found it important to examine junctions in three dimensions to exclude the terminals of MFs 14–1 and 14–2 in quantitative analyses, and because occasionally single confocal images that appeared to show a varicosity were misleading.

An artifactual swelling was seen at the NEP on occasion. It was observed in our specimens on the side of the animal on which the lateral incision was made, cutting the ISN roughly at the level of MF 4. This balloon-like structure could be distinguished from the prevaricosity because it had a nearly perfectly spherical shape, and its membrane often had a much weaker density of anti-HRP label, suggesting that it was swollen and stretched. In addition, a direct comparison between the cut side and the contralateral segment was quite striking.

Functional significance of the prevaricosity

The transition from growth cone to the varicosity stage was examined for maturity of functioning organelles. The development of a synapse-specific structure, namely a high density of synaptic vesicles, was examined with an antibody to synaptotagmin. Synaptotagmin is a membrane protein of synaptic vesicles

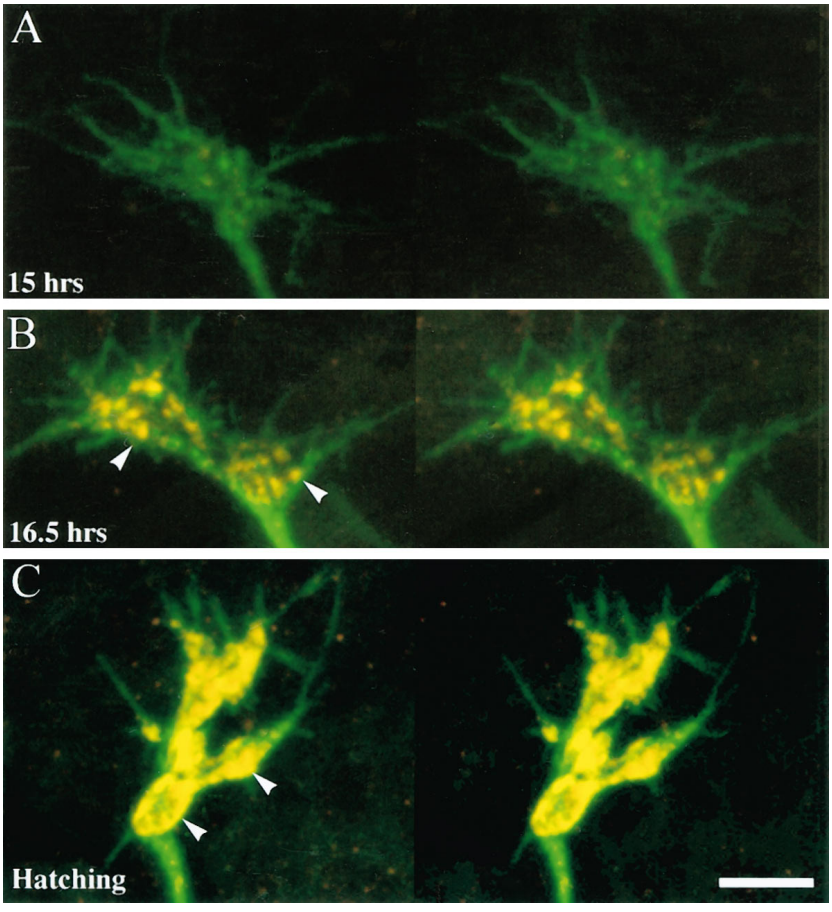

Figure 12. Development of anti-synaptotagmin immunoreactivity at synaptic terminals innervating MFs 1 and 9. The surface membranes of presynaptic nerve terminals were labeled with fluorescein-conjugated secondary antibodies to anti-HRP (*green*), and the synaptic vesicles were labeled with Cy-3-tagged antibodies to synaptotagmin (*red*). Each set is a stereo pair. *A*, There is little immunoreactivity to synaptotagmin (15 hr AEL), and the growth cones of the junctional aggregates are planar. *B*, Prevaricosity stage (16.5 hr AEL). Synaptotagmin immunoreactivity is clustered into discrete patches (*arrowheads*) within the prevaricosities. *C*, *Hatching* (21 hr AEL). Synaptotagmin immunoreactivity is denser, it is accumulated into larger patches, and the distribution of patches is restricted primarily to the outer margins of the varicosities (*arrowheads*).

and has been detected in *Drosophila* by 15 hr AEL in the flat growth cone (Littleton et al., 1993, 1995), as well as in later instars.

We examined the development of immunoreactivity to synaptotagmin from 15 hr AEL to hatching. Immunoreactivity was low during the flat growth cone stage but increased greatly in MFs 1 and 9 at 16.5 hr AEL (Fig. 12*B*). This increase was synchronous with the formation of the prevaricosity. The synaptotagmin labeling in the prevaricosity appeared in distinct patches located within the enlarged regions of the terminal near the muscle membrane. The discrete patches persisted into the stage of varicosity formation, with the density of each patch, as well as their number and size, increasing (Fig. 12*C*). The development of the axonal or terminal swelling at the prevaricosity is therefore presumably accompanied by an influx and a clustering of synaptic vesicles near developing active zones within the region. This interpretation is supported by TEM images that show clusters of vesicles, which increase in number and cluster dimensions from the prevaricosity period onward (Figs. 6, 9). The relative time courses of development of synaptotagmin immunoreactivity and prevaricosity formation, as well as other developmental features, are illustrated in Figure 13.

DISCUSSION

In growth cones, the axon terminal seems to be designed for elongation, exploration, target selection, and establishment of an adhesive association with a target. In the maturing presynaptic terminals on the body wall muscles of *Drosophila*, the transition from the growth cone stage to the varicose larval terminal is marked by an interim "prevaricosity" stage. The prevaricosities are larger than the varicosities so that, at least during embryonic development, varicosity formation results from constriction and subdivision of a larger structure rather than swelling of a smaller one. The prevaricosity stage begins between 15.5 and 16.5 hr

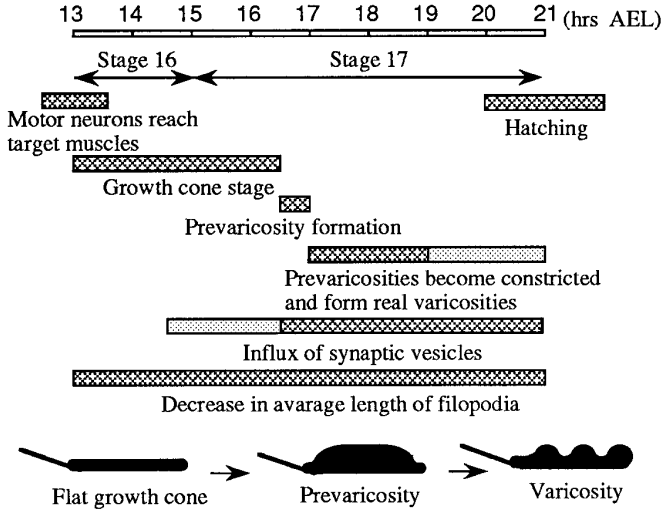

Figure 13. The approximate time course of the stages of development of the presynaptic terminals of MFs 1 and 9 at 25°C. Several aspects of development were explored. *Bars* represent the duration of each stage. The schematic drawings illustrate the changes in shape undergone by the terminals during this period. *Hatched regions* of *bars* indicate time when characteristic was the most obvious; *dotted regions* indicate time period when it was observed only occasionally, or less clearly.

AEL, depending on the specific MF. The prevaricosity stage is recognizable not only by an increase in the thickness of terminals at the NEP, but also by an influx of synaptotagmin-immunoreactive materials and the formation of synaptic specializations in them.

Labeling with anti-HRP or even antibodies specific to sets of motor neurons such as the antibody to Fas II (Schuster et al., 1996a) cannot accurately determine when the junctional aggregates include growth cones from all the different neurons that will come to innervate a particular muscle as opposed to several branches from a "pioneer" neuron. In MFs 6 and 7 at the time of prevaricosity formation, evoked junctional currents (Broadie and Bate, 1993) indicated that two separate excitatory axons were present as early as 16 hr AEL. Two axons were found in the cleft between MFs 6 and 7 at ~15 hr AEL, and ultrastructural evidence for synapse formation was seen by 16 hr AEL, which would be consistent with axons from both RP3 and 6/7b, the total mature innervation, being present by then (Schuster et al., 1996a). Our ultrastructural observations of MFs 1 and 9 similarly indicate that multiple axons are present in the nerve supplying MFs 1 and 9 by 16 hr AEL, and that this supply includes both Type I and Type II axons. It is still not known, however, the degree to which their arrival times may be staggered between 13 and 16 hr AEL.

In both 17 and 19 hr embryos we found several examples of putative nerve–nerve synapses, with presynaptic specializations, during the formation of the junctional aggregate at the NEP. They were consistently found at the NEP of MF 9 (sample of three animals) between the second profile and the first, with the first being in immediate contact with the MF and having the characteristics of a Type I terminal. The second axon sometimes contained dense-cored vesicles of the type occurring in the Type II axons or occasionally in Type Is (CVo) (Jia et al., 1993). The nature and function of these nerve–nerve synapses is unknown. It is possible that they represent a transient developmental phenomenon, that one of the three axons innervating MFs 1 and 9 is inhibitory in nature, or that the Type II terminals may on occasion form release sites in apposition to Type I terminals. Type II varicosities otherwise did not form morphologically discernible release sites in direct apposition to the sarcolemma in any of the animals sectioned so far. Prokop et al. (1996) recently reported ~3% neuro-neural synaptic contacts in a random sample of unidentified terminals in wild-type animals, which would be consistent with this type of synapse being found within other junctional aggregates in addition to those on MFs 1 and 9.

The description and time course of formation of varicosities in MFs 1 and 9 differ somewhat from that provided by Broadie and Bate (1993) in their study of MFs 6 and 7. This difference arises from two factors. First, we find that there are systematic differences in the rate at which junctions appear to form on the more dorsal muscles innervated by the ISN versus those on the ventral muscles innervated by branches of the SN. The developmental steps followed by MFs 1 and 9 seem to lag behind those of MFs 6 and 7 by ~0.5 hr. Second, we are using the term "varicosity" or "bouton" differently. We apply the term only to the 1–2 μm swellings that form at the base of the junction from the prevaricosity and house both clusters of vesicles and presynaptic dense bodies. The varicosities that they report at 14.5 hr AEL are very small swellings, ~0.2 μm in diameter (about the size of four synaptic vesicles), occurring along filopodia. Our observations would suggest that these small swellings are not necessarily the sites of the first boutons. Such small varicosities seen along filopodia or distal terminal branches may house releasable vesicles; however, in thin sections to date no presynaptic dense bodies have been found in them.

The mechanisms underlying determination of terminal shape and varicosity formation are largely unknown. The development of a normal number of varicosities during larval life is perturbed both by mutations that result in abnormal amounts of synaptic transmission and by mutations that affect adhesion molecules. These two factors appear to interact in complex ways. Double mutants having increased neuronal excitability (*ether-a-go-go, Shaker*), and thus increased neuromuscular activity, also form more varicosities by third instar (Budnik et al., 1990). These mutants also produce less of the adhesion molecule Fas II at their neuromuscular junctions (Schuster et al., 1996b). Direct involvement of Fas II in varicosity formation was demonstrated by examining mutants that have reduced levels of Fas II and by examining hyperexcitable *eag Sh* mutants with Fas II levels genetically maintained at normal levels in certain terminals (Schuster et al., 1996a,b).

These relationships are not straightforward: a 90% reduction in Fas II protein can give rise to terminals with *fewer* varicosities, but a 50% reduction gives rise to terminals with *more* varicosities (Schuster et al., 1996a). These direct and indirect effects of synaptic activity on varicosity formation occurred largely after hatching; differences in embryonic varicosity formation in the mutants were not noted, with even a mutant lacking Fas II developing some embryonic varicosities (Schuster et al., 1996a), so multiple mechanisms are likely to be involved in determining terminal shape.

Several factors may be involved in prevaricosity development. The first may be the manufacture or transport of synapse-specific components. The timing of prevaricosity formation coincides with a sudden increase in synaptotagmin immunolocalization within the terminal. If synaptic vesicles and other synaptic components are being transported down the axon to the terminal at the same time at which adhesive contacts are being made at the nerve muscle interface, swelling to form the prevaricosity might result. If so, then terminals innervating the ventral MFs 6 and 7 may swell in advance of those on the more dorsal muscles because of the shorter distance such synaptic components would have to travel along their respective axons.

Second, changes in the various types of cytoskeletal elements are likely to be involved. The decrease in filopodial length may involve loss or remodeling of actin bundles and change in microtubule distribution in the growth cone; the cytoplasm from retracted filopodia would then contribute to the enlarging prevaricosity. Precisely organized microtubules and intermediate filaments would subsequently be necessary for the formation of the elongated varicose shape and more permanent adhesions with the MF.

A third factor might be the interactions between the MF and the terminal itself. By the prevaricosity stage, some of the filopodia and other parts of the developing terminal lie beneath the basal lamina of the MF and are beginning to settle into depressions in the muscle surface. The MF responds locally to the presence of the nerve terminal by ruffling and forming processes that wrap it (Fig. 8 and additional unpublished observations). Such morphogenetic nerve–muscle interactions may also be involved in forming the constrictions.

Finally, Fas II, in addition to affecting varicosity formation, also affects axonal fasciculation (Lin et al., 1994). The degree to which

terminals in the embryo remain in intimate contact with each other during the early stages of junction formation, something that only gradually changes during the larval instars, was striking. Perhaps varicosity formation relies on modifying terminal–terminal interactions as well as nerve–muscle interactions.

The first pre- and postsynaptic specializations form in the prevaricosity along a broad contact region at the NEP. Because electrical events seem to be important in establishing and strengthening peripheral synapses (Colman et al., 1997), this would also be consistent with a hypothesis that both initial adhesive interactions and initial synaptic transmission help to determine final target specificity as well as terminal morphology.

There are relatively few descriptions of motor nerve terminal maturation in vertebrates or other invertebrates. Lupa and Hall (1989) report a distinctive stage (III) in which an oval accumulation of synaptic vesicle proteins was seen in an enlargement of the terminals of immature rodent neuromuscular junctions, with a distinctive complementary distribution of neurofilament proteins. This step seems to be comparable to the prevaricosity stage seen in *Drosophila* and may therefore represent an interesting stage in the maturation of all terminals.

REFERENCES

Anderson MD, Halpern ME, Keshishian H (1988) Identification of the neuropeptide transmitter proctolin in *Drosophila* larvae: characterization of muscle fiber-specific neuromuscular endings. J Neurosci 8:242–255.

Ashburner M (1989) *Drosophila*: a laboratory manual. Cold Spring Harbor, NY: Cold Spring Harbor Laboratory.

Atwood HL, Wojtowicz JM (1986) Short-term and long-term plasticity and physiological differentiation of crustacean motor synapses. Int Rev Neurobiol 28:275–362.

Atwood HL, Govind CK, Wu C-F (1993) Differential ultrastructure of synaptic terminals on ventral longitudinal abdominal muscles in *Drosophila* larvae. J Neurobiol 24:1008–1024.

Bate M (1990) The embryonic development of larval muscles in *Drosophila*. Development 110:791–804.

Broadie KS, Bate M (1993) Development of the embryonic neuromuscular synapse of *Drosophila melanogaster*. J Neurosci 13:144–166.

Broadie K, Prokop A, Bellen HJ, O'Kane CJ, Schulze KL, Sweeney ST (1995) Syntaxin and synaptobrevin function downstream of vesicle docking in *Drosophila*. Neuron 15:663–673.

Budnik V, Zhong Y, Wu C-F (1990) Morphological plasticity of motor axons in *Drosophila* mutants with altered excitability. J Neurosci 10:3754–3768.

Burns ME, Augustine GJ (1995) Synaptic structure and function: dynamic organization yields architectural precision. Cell 83:187–194.

Campos-Ortega JA, Hartenstein V (1985) The embryonic development of *Drosophila melanogaster*. Berlin: Springer.

Cantera R, Nassel DR (1992) Segmental peptidergic innervation of abdominal targets in larval and adult dipteran insects revealed with an antiserum against leucokinin I. Cell Tissue Res 269:459–471.

Colman H, Nabekura J, Lichtman JW (1997) Alterations in synaptic strength preceding axon withdrawal. Science 275:356–361.

Crossley AC (1978) The morphology and development of the *Drosophila* muscular system. In: The genetics and biology of *Drosophila*, Vol 2b (Ashburner M, Wright TRF, eds), pp 449–560. New York: Academic.

Goodman CS, Bastiani MJ, Doe CQ, du Lac S, Helfand SL, Kuwada JY, Thomas JB (1984) Cell recognition during neuronal development. Science 225:1271–1279.

Gorczyca M, Augart C, Budnik V (1993) Insulin-like receptor and insulin-like peptide are localized at neuromuscular junctions in *Drosophila*. J Neurosci 13:3692–3704.

Hall ZW, Sanes JR (1993) Synaptic structure and development: the neuromuscular junction. Cell 72/Neuron 10[Suppl]:99–121.

Halpern ME, Chiba A, Johansen J, Keshishian H (1991) Growth cone behavior underlying the development of stereotypic synaptic connections in *Drosophila* embryos. J Neurosci 11:3227–3238.

Harrison RG (1910) The outgrowth of the nerve fiber as a mode of protoplasmic movement. J Exp Zool 9:787–846.

Hertweck H (1931) Anatomie und Variabilität des Nervansystems und der Sinnesorgane von *Drosophila melanogaster* (Meigen). Z Wiss Zool 139:559–663.

Hoyle G (1955) The anatomy and innervation of locust skeletal muscle. Proc R Soc Lond [Biol] 143:281–292.

Jan LY, Jan YN (1976) L-glutamate as an excitatory transmitter at the *Drosophila* larval neuromuscular junction. J Physiol (Lond) 262:215–236.

Jan LY, Jan YN (1982) Antibodies to horseradish peroxidase as specific neuronal markers in *Drosophila* and grasshopper embryos. Proc Natl Acad Sci USA 72:2700–2704.

Jia X, Gorczyca M, Budnik V (1993) Ultrastructure of neuromuscular junctions in *Drosophila*: comparison of wild type and mutants with increased excitability. J Neurobiol 24:1025–1044.

Johansen J, Halpern ME, Johansen KM, Keshishian H (1989a) Stereotypic morphology of glutamatergic synapses on identified muscle cells of *Drosophila* larvae. J Neurosci 9:710–725.

Johansen J, Halpern ME, Keshishian H (1989b) Axonal guidance and the development of muscle fiber-specific innervation in *Drosophila* embryos. J Neurosci 9:4318–4332.

Katz F, Moats W, Jan YN (1988) A carbohydrate epitope expressed uniquely on the cell surface of *Drosophila* neurons is altered by the mutant *nac* (neurally altered carbohydrate). EMBO J 7:3471–3477.

Keshishian H, Chiba A, Chang TN, Halfon MS, Harkins EW, Jarecki J, Wang L, Anderson MD, Cash S, Halpern ME, Johansen J (1993) Cellular mechanisms governing synaptic development in *Drosophila melanogaster*. J Neurobiol 24:757–787.

Kelley RD, Dekker RAF, Bluemink JG (1973) Ligand-mediated osmium binding: its application in coating biological specimens for scanning electron microscopy. J Ultrastruct Res 45:254–258.

Kidokoro Y, Nishikawa K (1994) Miniature endplate currents at the newly formed neuromuscular junction in *Drosophila* embryos and larvae. Neurosci Res 19:143–154.

Kurdyak P, Atwood HL, Stewart BA, Wu C-F (1994) Differential physiology and morphology of motor axons to ventral longitudinal muscles in larval *Drosophila*. J Comp Neurol 350:463–472.

Lin DM, Fetter RD, Kopczynski C, Grenningloh G, Goodman CS (1994) Genetic analysis of Fasciclin II in *Drosophila*: defasciculation, refasciculation, and altered fasciculation. Neuron 13:1055–1069.

Littleton JT, Bellen HJ, Perin MS (1993) Expression of synaptotagmin in *Drosophila* reveals transport and localization of synaptic vesicles to the synapse. Development 118:1077–1088.

Littleton JT, Upton L, Kania A (1995) Immunocytological analysis of axonal outgrowth in synaptotagmin mutations. J Neurochem 65:32–40.

Lupa MT, Hall ZW (1989) Progressive restriction of synaptic vesicle protein to the nerve terminal during development of the neuromuscular junction. J Neurosci 9:3937–3945.

Monastirioti M, Gorczyca M, Rapus J, Eckhart M, White K, Budnik V (1995) Octopamine immunoreactivity in the fruit fly *Drosophila melanogaster*. J Comp Neurol 356:275–287.

Nishikawa K, Kidokoro Y (1995) Junctional and extrajunctional glutamate receptor channels in *Drosophila* embryos and larvae. J Neurosci 15:7905–7915.

Prokop A, Landgraf M, Rushton E, Broadie K, Bate M (1996) Presynaptic development at the *Drosophila* neuromuscular junction: assembly and localization of presynaptic active zones. Neuron 17:617–626.

Ramon y Cajal S (1890) A quelle epoque apparaissent les expansions des cellules nerveuses de la moelle epiniere du poulet? Anat Ang 5:609–613.

Rheuben MB, Reese TS (1978) Three-dimensional structure and membrane specializations of moth excitatory neuromuscular synapse. J Ultrastruct Res 65:95–111.

Schaner PJ, Rheuben MB (1985) Scanning and freeze-fracture study of larval nerves and neuromuscular junctions in *Manduca sexta*. J Neurobiol 16:83–96.

Schuster CM, Davis GW, Fetter RD, Goodman CS (1996a) Genetic dissection of structural and functional components of synaptic plasticity. I. Fasciclin II controls synaptic stabilization and growth. Neuron 17:641–654.

Schuster CM, Davis GW, Fetter RD, Goodman CS (1996b) Genetic dissection of structural and functional components of synaptic plasticity. II. Fasciclin II controls presynaptic structural plasticity. Neuron 17:655–667.

Sink H, Whitington PM (1991) Location and connectivity of abdominal motoneurons in the embryo and larva of *Drosophila melanogaster*. J Neurobiol 22:298–311.

Snow PM, Patel NH, Harrelson AL, Goodman CS (1987) Neural-specific carbohydrate moiety shared by many surface glycoproteins in *Drosophila* and grasshopper embryos. J Neurosci 7:4137–4144.

Sonea IM, Rheuben MB (1992) Degenerative changes in the function of neuromuscular junctions of *Manduca sexta* during metamorphosis. J Exp Biol 167:61–89.

Stewart BA, Atwood HL, Renger JJ, Wang J, Wu C-F (1994) Improved stability of *Drosophila* larval neuromuscular preparations in haemolymph-like physiological solutions. J Comp Physiol [A] 175:179–181.

Stewart BA, Schuster CM, Goodman, CS, Atwood HL (1996) Homeostasis of synaptic transmission in *Drosophila* with genetically al-.tered nerve terminal morphology. J Neurosci 16:3877–3886.

Usherwood PNR (1974) Nerve-muscle transmission. In: Insect neurobiology (Treherne JE, ed), pp 245–305. Amsterdam: North Holland.

Van Vactor D, Sink H, Fambrough D, Tsoo R, Goodman CS (1993) Genes that control neuromuscular specificity in *Drosophila*. Cell 73:1137–1153.

Wood JI, Klomparens KL (1993) Characterization of agarose as an encapsulation medium for particulate specimens for transmission electron microscopy. Microsc Res Tech 25:267–275.

Zhong Y, Budnik V, Wu C-F (1992) Synaptic plasticity in *Drosophila* memory and hyperexcitable mutants: role of cAMP cascade. J Neurosci 12:644–651.